2013

The Hyaluronan Receptor for Endocytosis (HARE) Activates NF-κB-mediated Gene Expression in Response to 40–400-kDa, but Not Smaller or Larger, Hyaluronans

Madhu S. Pandey
University of Oklahoma Health Sciences Center

Bruce A. Baggenstoss
University of Oklahoma Health Sciences Center

Jennifer Washburn
University of Oklahoma Health Sciences Center

Edward N. Harris
University of Nebraska-Lincoln, eharris5@unl.edu

Paul H. Weigel
University of Oklahoma Health Sciences Center, paul-weigel@ouhsc.edu

THE JOURNAL OF BIOLOGICAL CHEMISTRY VOL. 288, NO. 20, pp. 14068–14079, May 17, 2013

The Hyaluronan Receptor for Endocytosis (HARE) Activates NF-κB-mediated Gene Expression in Response to 40–400-kDa, but Not Smaller or Larger, Hyaluronans*[S]

Received for publication, December 6, 2012, and in revised form, March 13, 2013 Published, JBC Papers in Press, March 24, 2013, DOI 10.1074/jbc.M112.442889

Madhu S. Pandey[‡], Bruce A. Baggenstoss[‡], Jennifer Washburn[‡], Edward N. Harris[§], and Paul H. Weigel[‡1]

From the [‡]Department of Biochemistry and Molecular Biology, Oklahoma Center for Medical Glycobiology, University of Oklahoma Health Sciences Center, Oklahoma City, Oklahoma 73104 and the [§]Department of Biochemistry, University of Nebraska, Lincoln, Nebraska 68588

Background: HARE mediates systemic clearance of hyaluronan (HA), which turns over continuously in tissues.
Results: HARE uptake of 40–400-kDa, but not larger or smaller, HA stimulated NF-κB activation.
Conclusion: HA-HARE signal complexes activate NF-κB and gene transcription only with optimally sized HA.
Significance: HARE responsiveness to a narrow size range of HA degradation products may be a sensing system to detect tissue ECM stress.

The hyaluronan (HA) receptor for endocytosis (HARE; Stabilin-2) binds and clears 14 different ligands, including HA and heparin, via clathrin-mediated endocytosis. HA binding to HARE stimulates ERK1/2 activation (Kyosseva, S. V., Harris, E. N., and Weigel, P. H. (2008) *J. Biol. Chem.* 283, 15047–15055). To assess a possible HA size dependence for signaling, we tested purified HA fractions of different weight-average molar mass and with narrow size distributions and Select-HA™ for stimulation of HARE-mediated gene expression using an NF-κB promoter-driven luciferase reporter system. Human HARE-mediated gene expression was stimulated in a dose-dependent manner with small HA (sHA) >40 kDa and intermediate HA (iHA) <400 kDa. The hyperbolic dose response saturated at 20–50 nM with an apparent K_m ~10 nM, identical to the K_d for HA-HARE binding. Activation was not detected with oligomeric HA (oHA), sHA <40 kDa, iHA >400 kDa, or large HA (lHA). Similar responses occurred with rat HARE. Activation by sHA-iHA was blocked by excess nonsignaling sHA, iHA, or lHA, deletion of the HA-binding LINK domain, or HA-blocking antibody. Endogenous NF-κB activation also occurred in the absence of luciferase plasmids, as assessed by degradation of IκB-α. ERK1/2 activation was also HA size-dependent. The results show that HA-HARE interactions stimulate NF-κB-activated gene expression and that HARE senses a narrow size range of HA degradation products. We propose a model in which optimal length HA binds multiple HARE proteins to allow cytoplasmic domain interactions that stimulate intracellular signaling. This HARE signaling system during continuous HA clearance could monitor the homeostasis of tissue biomatrix turnover throughout the body.

Hyaluronan (HA),[2] a ubiquitous extracellular matrix (ECM) component, is synthesized by many different cell types as a large co-polymer of -GlcNAc(β1,4)GlcUA(β1,3)- disaccharides, typically in the MDa mass range. This large HA has general functions in matrix structural integrity, water and cation homeostasis in all tissues, and specialized functions in some tissues, such as a lubricant in synovial fluid (1). HA binds to many different hyaladherins (2), HA-binding proteins, involved in remodeling and organizing ECM in a tissue-specific fashion (3). HA binding to surface receptors activates cell signaling events important for development, wound healing, and metastasis of some cancers (4–7).

Among biopolymers, the polydispersity of HA (*i.e.* weight-average mass ÷ number-average mass; M_w/M_n) in biological samples is exceptional. Sizes range in length from 4 to 50,000 sugars. Literature terms for HA size are not uniform or consistent, and some reports use identical terms (*e.g.* small) for different sizes (8). To facilitate data presentation and discussion (Fig. 1), we use four designations to define HA size ranges (oHA, sHA, iHA, and lHA) based on a five log-scale size range with three log boundaries (at 10, 100, and 1,000 kDa). For example, large HA (lHA; >1–10 MDa) in the ECM can be depolymerized to intermediate HA (iHA; >100–1,000 kDa), small HA (sHA; >10–100 kDa), and oligomeric HA (oHA; 1–10 kDa) during various normal or pathophysiological situations such as tissue injury, tumorigenesis, bacterial infection, oxidative stress, or exposure to reactive oxygen intermediates at the site of inflammation (9–14).

sHA and lHA promote different cellular and biological responses. lHA can prevent scar formation during fetal wound healing and in spinal cord injuries. These biological activities

* This work was supported, in whole or in part, by National Institutes of Health Grant GM69961 from NIGMS. This work was also supported by OCAST Grant HR10-074 from the State of Oklahoma.
[S] This article contains supplemental Figs. S1–S5.
[1] To whom correspondence should be addressed: Tel.: 405-271-1288; Fax: 405-271-3092; E-mail: paul-weigel@ouhsc.edu.

[2] The abbreviations used are: HA, hyaluronic acid, hyaluronate, hyaluronan; Ab, antibody (IgG); EV, empty vector; ECM, extracellular matrix; HARE, hyaluronic acid receptor for endocytosis; hHARE, 190-kDa human HARE; rHARE, rat HARE; iHA, intermediate HA (>100 to 1,000 kDa); LMW-HA, low molecular weight HA; lHA, large (>1 MDa) HA; luc, luciferase; MALLS, multiangle laser light scattering; M_w, weight-average molar mass; sHA, small HA (>10 to 100 kDa); oHA, oligosaccharide HA (>1 to 10 kDa); SEC, size-exclusion chromatography; Stab2, Stabilin-2; CS, chondroitin sulfate.

occur in various cell types as altered cell proliferation, infiltration, or glycosaminoglycan synthesis (15, 16). oHA or sHA can activate cell proliferation, differentiation, or angiogenesis (17, 18). In rheumatoid arthritis, sHA fragments, generated by degradation of native lHA from synovial fluid, interact with TLR-2 and TLR-4 and modulate inflammatory mechanisms (19).

NF-κB is a ubiquitously expressed transcription factor that plays important roles in regulating many genes encoding proinflammatory cytokines, chemokines, growth factors, and adhesion molecules (20). NF-κB is activated by many inflammatory and cell stress stimuli, including cytokines (*e.g.* TNF-α and IL-1β), mitogens, environmental particles, toxic metals, pathogens, and pathogen-derived products (21). Normally, in the cytoplasm, activated NF-κB translocates to the nucleus, binds to the promoter of the targeted genes, and activates their transcription. Activation of NF-κB is a hallmark indicator in the acute phase of inflammatory response after injury or infection (22). Binding of sHA, but not lHA, to CD44 significantly increases production of the inflammatory cytokine IL-6 (23). In 3LL and embryonic fibroblasts, oHA strongly stimulates NF-κB activation by an unknown HA receptor and induces expression of metalloproteases MMP-9 and MMP-13 (24).

HARE, which begins at Ser^{1135} and ends at the C-terminal Leu^{2551} of full-length Stab2 (25, 26), is a 190-kDa fully functional isoform of Stab2 that is generated by proteolysis (27); it is preferentially and highly expressed in the sinusoidal endothelial cells of liver and lymph node (26, 28–30), the tissues responsible for systemic HA clearance. We designate the full-length 315-kDa protein as Stab2 and HARE as the 190-kDa isoform that is not a splice variant. HARE and Stab2 function as primary scavenger receptors for systemic clearance of 14 different ligands, and other functions, including cell signaling, have only recently been examined. We found that HA binding to HARE can stimulate cell signaling, leading to activation of the MAPK ERK1/2 in a dose- and time-dependent manner (31). Park *et al.* (32) found stimulation of anti-inflammatory cytokine release in macrophages phagocytosing apoptotic cells via the phosphatidylserine binding activity of these proteins.

HARE was first characterized by Laurent, Fraser, and coworkers (4, 33–35) as a systemic clearance receptor that removes HA and chondroitin sulfate (CS) from the vascular and lymphatic circulatory systems. Adult humans contain ~15 g of tissue HA and synthesize and degrade one-third of this amount daily. Native lHA is continuously partially degraded by an unknown mechanism and released from tissue ECMs as ~1-MDa fragments that may contain bound proteins such as growth factors and lecticans with CS and other glycosaminoglycan chains (31–33). These HA-proteoglycan fragments and associated components enter the lymphatics and lymph nodes, the initial and primary sites for 85% of the HA and CS clearance and degradation. Liver is the second clearance site, after the lymph node effluent enters the circulation, accounting for 15% of the total body HA and CS turnover. HARE/Stab2 is also highly expressed in sinusoidal endothelial cells of spleen (26) and bone marrow (36), perhaps mediating local HA turnover, and is also found in macrophages (32), corneal and lens epithelium, mesenchymal heart valve cells, ependymal brain ventricle cells, prismatic epithelial cells covering renal papillae, and oviduct (37).

Here, we used NF-κB promoter-driven Dual-Luciferase gene expression to test HA preparations of different sizes for their ability to stimulate HARE-mediated gene expression in stable HEK Flp-In 293 cell lines. HA binding to rat or human HARE stimulated NF-κB-mediated gene expression in a dose- and time-dependent way. This response was very dependent on HA size, only occurring with a narrow size range at the sHA-iHA boundary (40–400 kDa); smaller oHA or sHA and larger sHA, iHA, or lHA were inactive. The optimum signaling size was ~140 kDa. This HARE receptor signaling system in response to HA clearance could play a role in monitoring the status of tissue biomatrix turnover throughout the body.

EXPERIMENTAL PROCEDURES

Cells, Plasmids, and Reagents—Flp-In 293 cells, FBS, DMEM, hygromycin B, Zeocin, Lipofectamine 2000, Lipofectamine LTX and PLUS reagents, glutamate, plasmid expression vectors, and super-competent TOP10 *Escherichia coli* were from Invitrogen. Plasmid vectors pGL4.32(luc2P/NF-κB-RE/Hygro), Dual-Luciferase Reporter Assay System (E1960), and Luminometer Glomax 20/20 were from Promega (Madison, WI). Plasmid pRL-TK was kindly provided by Dr. K. Mark Coggeshall (Oklahoma Medical Research Foundation). Stable cell lines expressing HARE and HARE mutants were generated as described previously (25, 31) using Flp-In 293 (HEK) cells, which are engineered to contain a selected recombinase insertion site, and the correct single insertion was verified. The Invitrogen protocol was followed to confirm that the clones selected contained one transgene inserted at the correct locus. End-labeled ^{3}H-oligosaccharides of identical specific activity were a generous gift from Dr. Paul DeAngelis. Rabbit anti-phospho-ERK1/2 (p44/42; $Thr(P)^{202}$ and $Tyr(P)^{204}$), rabbit anti-ERK1/2, and mouse anti-IκB-α monoclonal Ab were from Cell Signaling Technology, Inc. (St. Louis, MO). Goat anti-rabbit IgG-HRP, donkey anti-goat IgG-HRP, and donkey anti-mouse IgG-HRP were from Santa Cruz Biotechnology (Santa Cruz, CA). Mouse monoclonal Ab6276 to human β-actin was from Abcam (Cambridge, MA).

Limulus amebocyte lysate reagent (Endosafe KTA 0.03 endotoxin units/ml) was from Charles River (Charleston, SC). HA prepared by bacterial fermentation was obtained from Genzyme Corp. (Cambridge, MA) or Lifecore (Chaska, MN). Select-HA™ was from Hyalose (Oklahoma City, OK). Protease inhibitor mixture (4-(2-aminoethyl)benzenesulfonyl fluoride, aprotinin, leupeptin, bestatin, pepstatin A, and E-64), sodium pyrophosphate, sodium fluoride, sodium orthovanadate, benzamidine, 2-mercaptoethanol, EGTA, EDTA, Tween 20, Sephacryl resins, and Trace Select grade ammonium acetate (catalogue 73432) were from Sigma. Enhanced chemiluminescence (ECL) substrate was from PerkinElmer Life Sciences. Optimum Brand autoradiography film was from Life Sciences Products (Frederick, CO), and nitrocellulose membranes were from Schleicher & Schuell. Other materials, reagents, and kits were obtained as described recently (38) or were from Sigma. The compositions of PBS, Lysis Buffer, TBST (TBST, Tris-buffered saline with Tween 20), and other buffers were as described pre-

viously (31, 38) Compete Medium contained DMEM supplemented with 8% FBS and 100 μg/ml hygromycin B. Transfection medium contained DMEM with 8% FBS (no antibiotics). Protein content was determined by the Bradford method (39) using BSA as the standard.

Preparation and Characterization of Defined Size, Low Endotoxin HA—Preparations of sHA (with M_w = 36, 66, or 80 kDa) and iHA (with M_w = 107, 178, 436, 549, or 967 kDa) with narrow size distributions and minimal overlap were purified by size-exclusion chromatography (SEC) and characterized by SEC-multiangle laser light scattering (SEC-MALLS) analysis. HA to be fractionated was either variable broad size range HA (Lifecore) or MDa size HA (Genzyme) subjected to mild acid hydrolysis, under conditions that did not cleave *N*-acetyl groups (*e.g.* 0.05 N HCl at 55 °C for 1–4 h), and then neutralized. All glassware was either treated with 0.5 N NaOH or baked at 250 °C overnight. Low trace-metal ammonium acetate minimized metal ion content after lyophilization, and ethanol was included in buffers to minimize bacterial contamination. Samples were fractionated over Sephacryl HR-500 (for HA >400 kDa) or HR-400 (for HA <400 kDa) columns (3.7 × 120 cm; 1.3-liter bed volume). A Gilson PrepFC fraction collector was housed in a custom Plexiglass box to minimize dust entering the tubes. Positive pressure was maintained using an aquarium pump by air flowing through a vacu-guard filter. The elution buffer was 50 mM ammonium acetate containing 20% ethanol, and 7.5-ml fractions were collected. Portions of every third fraction were analyzed by MALLS for HA size distribution, concentration, and M_w (40). Groups of three fractions from ≥5 identical runs were pooled based on their MALLS profiles and lyophilized using Triforest Duocap flasks (ISC Bioexpress, Kaysville, UT). Pellets were dissolved in 2 ml of sterile deionized water and transferred to a 15-ml conical polypropylene tube. Sterile deionized water (4 ml) was added to the flasks, which were rocked at room temperature for 2 h to recover residual HA. The pooled 6-ml solution was filtered using a 0.2-μm polyethersulfone sterile syringe filter, lyophilized, dissolved in 2 ml of sterile deionized water, and lyophilized again. Samples taken from the pools were assessed for endotoxin using the *Limulus* amebocyte lysate assay and analyzed by SEC-MALLS to determine final HA concentrations, M_w, and size distributions. Endotoxin levels in all purified HA samples were <1 endotoxin units/mg. HA concentrations are expressed in molar units based on weight-average mass (because this is usually provided by all vendors); values are not corrected for differences between weight-average and number-average mass.

Agarose Gel Electrophoresis—HA samples (1–3 μg/lane) were analyzed by agarose gel electrophoresis using 0.8–1.5% gels in TAE buffer (41) at 80–90 V for 2–3 h with the apparatus in an ice bath. Gels were stained overnight with 0.005% Stains-All in 50% ethanol, destained by washing in water and exposed to light, and then digitally scanned and photographed.

Cell Culture and Transient Transfection—Flp-In 293 cells stably expressing 190-kDa human HARE (hHARE), rat HARE (rHARE), hHARE lacking the Link domain (hHARE(ΔLink)), or empty vector (EV) were grown to confluence in Complete Medium, plated in 12-well tissue culture plates, and maintained in Complete Medium for at least 2 days prior to experiments. At 50–60% confluence, Transfection Medium was added 10 min prior to transfection. Transfection complexes were generated in serum-free medium by mixing Lipofectamine LTX and PLUS reagents with 1 μg/ml firefly luciferase (LUC) vector pGL4.32(luc2P/NF-κB-RE/Hygro) and 0.5 μg/ml pRL-TK (*Renilla* luciferase vector). Transiently transfected cells were grown for 18 h before use.

HA Treatment of Stable Cell Lines—Cells expressing 190-hHARE, 190-rHARE, and 190-hHARE mutants or EV were transiently transfected with firefly and *Renilla* LUC vectors as above, washed once each with sterile PBS and DMEM without serum, and then preincubated with fresh serum-free DMEM for 1 h at 37 °C. To determine the time dependence for HA-HARE-mediated NF-κB activation of reporter gene expression, hHARE cells were incubated with 125 nM 80-kDa sHA for 3, 4, or 6 h (supplemental Fig. S1). Because no significant differences were seen between 3 and 6 h, we performed all experiments (to assess HA concentration and mass dependence of HARE-mediated NF-κB-activated gene expression) using a 1-h pretreatment and a 4-h treatment period (to allow ample time for gene expression and protein translation). The medium was then aspirated, and cells were processed to determine the extent of NF-κB-activated reporter gene expression (see below).

Dual-Luciferase Reporter Assays and Analysis of NF-κB Activity—After cell stimulation with HA, or TNF-α (positive control), cells were washed with sterile PBS, scraped, and harvested in serum-free medium. Cells were centrifuged at 12,000 × *g* for 1 min; supernatants were aspirated, and pellets were resuspended in 150 μl of serum-free medium and assayed for LUC activities using the Dual-Luciferase Reporter Assay System following the manufacturer's protocol (Promega). The amounts of firefly and *Renilla* LUC activities in each sample were measured and recorded as relative light units using a Glomax 20/20 luminometer (Promega). The ratio of firefly luciferase to *Renilla* LUC activity in each condition was calculated and normalized to the value for untreated control cells (defined as 1.0). Results are expressed as mean ± S.E. fold-change in firefly/*Renilla* LUC activity.

Analysis of Phospho-ERK1/2—EV or hHARE cells were grown to confluence in Complete Medium, washed with sterile PBS, and serum-starved for 1 h followed by incubation with 560- or 80-kDa HA for the indicated times. Cells were processed for ERK1/2 activation as described (31).

IκB Degradation Assay—EV or hHARE cells were grown to confluence in 6-well plates, washed with sterile PBS, and then incubated with serum-free DMEM for 1 h. Cells were stimulated with 1 ng/ml TNF-α or 100 nM HA (137 kDa) for the indicated times. Equal amounts of cell lysate protein, made as above, were run on 10% SDS-PAGE, transferred to nitrocellulose, and then probed with anti-IκB Ab.

Statistical Analysis—Values are presented as the mean ± S.E. based on three independent experiments performed in triplicate (n = 9), unless noted otherwise. Data to be compared were first analyzed by a one-way analysis of variance, and any significant difference in the group was then assessed by individual pairwise post hoc Tukey's HSD tests using GraphPad Prism v6 statistical software (GraphPad Software, Inc., San Diego). Pairwise comparisons were made for EV and HARE cells with the

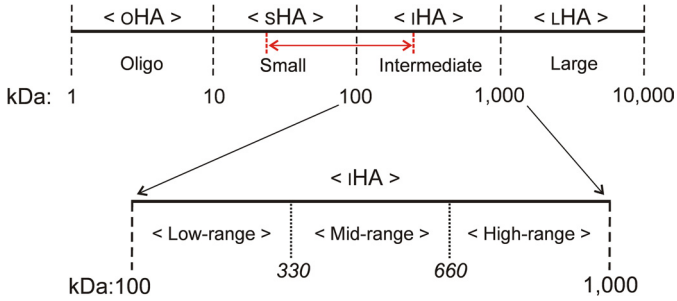

FIGURE 1. **HA size nomenclature based on log incremental mass ranges.** Four different 10-fold HA mass ranges are used (*top of panel*) as follows: oHA (between >1 and 10 kDa); sHA (between >10 and 100 kDa); iHA (between >100 and 1,000 kDa), and lHA (between >1,000 and 10,000 kDa). HA size within any of these four mass ranges is described further by assigning thirtiles (one-thirds) by the descriptors low-, mid-, and high-range. For example (*bottom of panel*), sizes within the iHA range are further defined as low-range (100–330 kDa), mid-range (330–660 kDa), and high-range (660–999 kDa) iHA. The smallest oHA fragment is actually a tetrasaccharide (technically <1 kDa), and the largest HA size *in vivo* is unknown but is likely >10 MDa (>lHA). The *red dotted lines* and spanning *double-arrow* represent the sHA-iHA region of active HA (~40–400 kDa) capable of stimulating HARE-mediated signaling and gene activation.

same HA concentration and then with HARE cells plus HA *versus* EV cells without HA. Only those sample sets with significant differences in both cases are marked (values considered statistically significant were as follows: *, $p < 0.05$; **, $p < 0.005$; ***, $p < 0.001$; ****, $p < 0.0001$).

RESULTS

Native high mass MDa lHA is broken down to smaller size HA (oHA, sHA, or iHA) during various pathophysiological situations that generate free radicals or increase hyaluronidase activities, *e.g.* during tissue injury, oxidative stress, infections, tumorigenesis, or exposure to reactive oxygen species at inflammation sites (12–14). Intact native HA is generally designated high molecular weight HA (despite use of the term molecular weight being technically incorrect, because mass units are almost always given, and there is no true molecular weight for polydisperse HA preparations). The HA field lacks a standard nomenclature to define and designate the broad size ranges of HA found physiologically. For example, some reports (43) designated 500-kDa HA as low molecular weight HA, whereas others consider the same size to be high molecular weight HA. To minimize confusion here, we utilize an HA size nomenclature based on a five-log scale of mass ranges from 1 kDa to 10 MDa (Fig. 1).

SEC-MALLS Analyses of HA Size and Concentration—Various HA preparations of M_w from 14 to 967 kDa were purified by SEC fractionation and selective pooling from replicate column runs, based on SEC-MALLS analysis of column fractions. Fractions with similar HA sizes were pooled, and the final preparations were analyzed for size distribution, HA concentration, and M_w. SEC-MALLS simultaneously provides these data for each sample analyzed (40, 44). This approach enabled preparative scale production of narrow size range HA preparations, with low polydispersity. For example, the polydispersities of Genzyme and Lifecore HA used here were 1.2 and 1.3, respectively, whereas the sHA (36, 66, and 80 kDa), low-range iHA (107 and 178 kDa), and the mid- and high-range iHA (436, 549, and 967 kDa) preparations had polydispersities of 1.05–1.15

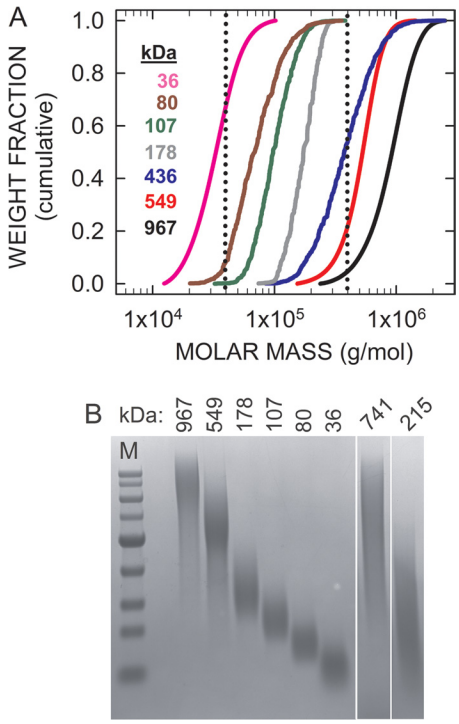

FIGURE 2. **SEC-MALLS and electrophoretic analyses of purified HA preparations.** Non-animal-derived, low endotoxin-containing HA preparations were fractionated by SEC and selectively pooled as described under "Experimental Procedures." *A,* size distribution for each color-coded HA preparation with the indicated M_w (ranging from 36 to 967 kDa) is plotted as the cumulative weight fraction. The sizes within the *vertical dotted lines* represent the active HA size range for HARE-mediated stimulation of NF-κB activated gene expression. *B,* agarose gel electrophoresis of the indicated purified narrow size range HA preparations was performed and the 1.2% gels processed as described under "Experimental Procedures." For comparison, unfractionated HA preparations (LifeCore) with M_w values of 741 and 215 kDa are shown at the *right*. The M_w values for Lo- and High-Ladder Select-HA standards in *lane M* were (kDa) as follows: 30.3, 111, 214, 310, 495, 667, 940, 1138, and 1510.

(*i.e.* a value of 1.0 is a monodisperse polymer). Each HA preparation showed minimal or no overlap with several larger or smaller preparations based on SEC-MALLS cumulative weight fraction (Fig. 2*A*) or agarose gel electrophoretic (Fig. 2*B*) analysis (*e.g.* most low-range iHA fractions do not overlap with high-range iHA fractions). Importantly, all HA preparations had endotoxin levels of <1 endotoxin unit/mg and, as noted in the experiments below, did not stimulate signaling in control EV cells.

Many studies have described differential effects of sHA *versus* lHA in cell signaling to promote different biological activities (8, 45–47); thus, it is clear that sHA and iHA are physiologically important inducers of various cell signaling pathways, including HA-HARE-mediated ERK1/2 activation (31). To study the HA size dependence of HARE-mediated signaling, we used an NF-κB promoter-driven Dual-Luciferase reporter assay system to determine whether downstream gene expression changes could be an outcome of a signaling pathway (48). Various endogenous inflammatory stimuli (*e.g.* cytokines, TNF-α, and IL-1β) or bacterially derived substances (*e.g.* lipopolysaccharide) activate the NF-κB pathway and promote downstream-targeted gene expression. To test whether our recombinant Flp-In 293 cell lines respond to TNF-α (a cytokine that activates NF-κB-mediated gene expression), we incubated

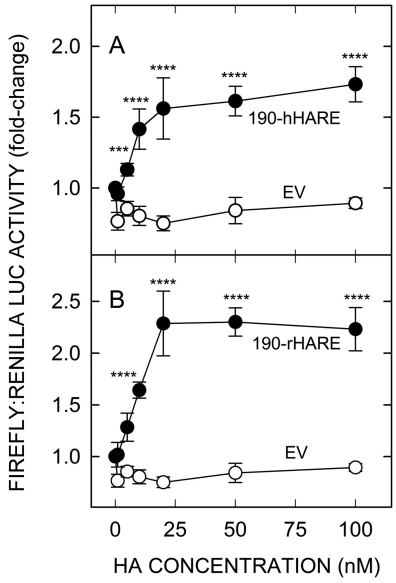

FIGURE 3. **HA binding to human or rat HARE mediates NF-κB-activated gene expression in a dose-dependent manner.** Cells expressing hHARE (*A*, ●), rHARE (*B*, ●) or EV (*A* and *B*; ○) were grown and transiently transfected with plasmids encoding firefly and *Renilla* LUC for 18 h in Transfection Medium. Cells were washed, incubated in serum-free medium for 1 h, washed again, and incubated with the indicated concentrations of 107-kDa iHA for 4 h. Cells were then processed and analyzed for their relative ratios of LUC activities as described under "Experimental Procedures." Results are normalized to the untreated control and expressed as a fold-change in the ratio of firefly-to-*Renilla* LUC activity. In Figs. 3–9, values are means ± S.E. ($n = 9$) from three independent experiments, unless noted otherwise. Values for *p* compare HARE and EV cells at each HA concentration and HARE cells plus HA *versus* EV cells without HA. Only sample sets with significant differences in both cases are marked: ***, $p < 0.001$; ****, $p < 0.0001$.

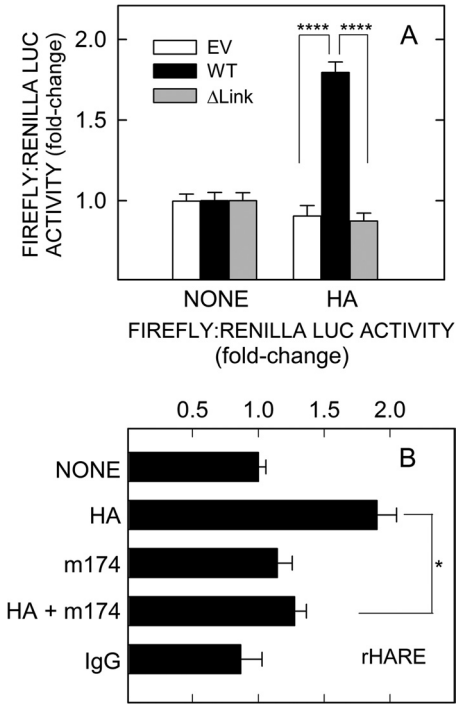

FIGURE 4. **HA-HARE binding is required for NF-κB-activated gene expression.** *A*, cells expressing hHARE (*black bars*), hHARE(ΔLink) (*gray bars*), or EV (*white bars*) were incubated with nothing or 50 nM 107-kDa HA and processed as in Fig. 3 (****, $p < 0.0001$; $n = 9$). *B*, cells expressing rHARE were incubated with 50 nM 107-kDa HA, 30 μg/ml mAb-174 mAb, or mouse IgG alone for 4 h and/or with HA added after preincubation with mAb-174 for 30 min and then processed as in Fig. 3 (*, $p < 0.05$; $n = 9$).

EV or hHARE cells with increasing concentrations of TNF-α. Both cell lines showed NF-κB activation of firefly luciferase gene expression in a dose-dependent manner (supplemental Fig. S2). The similar level of reporter gene expression in EV and hHARE cells indicates that these 293-derived cells are capable of activating this model reporter gene pathway and that, as expected, HARE is not required.

HA Binding to Human or Rat HARE Activates NF-κB-mediated Gene Expression in a Dose-dependent Manner—A sequence alignment of human, rat, and mouse HARE proteins (supplemental Fig. S3; the C-terminal 44% of Stab2) shows the human and rat sequences are 77% identical (28). To determine whether HA binding to rat or human HARE stimulates NF-κB activation, we incubated stable Flp-In 293 cell lines expressing rHARE, hHARE, or EV with increasing concentrations of 107-kDa iHA for 4 h (Fig. 3). Both human (Fig. 3*A*) and rat (Fig. 3*B*) HARE activated NF-κB-mediated reporter gene expression in an essentially identical HA dose-dependent manner. Both receptors showed surprisingly high sensitivity to HA, with significant activation at minimal doses of 5 and 10 nM, compared with EV cells ($p < 0.0001$). Human and rat HARE showed similar 1.7–2.3-fold increases in NF-κB activation at saturation, above 20 nM. Importantly, the dose response for each HARE species was hyperbolic with an apparent K_m of ~10 nM, which is nearly identical to the dissociation constants for HA-HARE complexes in cells expressing recombinant receptor (*e.g.* K_d ~7 nM) or purified ectodomain (*e.g.* K_d ~10–20 nM) protein (25, 27).

HA Binding to HARE Is Required for NF-κB-activated Gene Expression—HARE contains a 93-amino acid Link domain, which is required for HA binding and for HA-HARE-mediated ERK1/2 activation (31). Deletion of the Link domain inhibits HA binding and internalization by >90% compared with wild type hHARE and abolishes ERK1/2 activation. To verify that HA binding to hHARE is required for NF-κB-activated gene expression, we treated EV, hHARE, and hHARE(ΔLink) cells with 50 nM HA (107 kDa) for 4 h. HA did not stimulate NF-κB-activated gene expression in either EV or hHARE(ΔLink) cells (Fig. 4*A*), compared with hHARE cells ($p < 0.0001$). A positive control using TNF-α showed identical LUC activation in all three cell lines, demonstrating that 190-hHARE(ΔLink) cells have a functional signaling pathway (data not shown). The results confirm that HA binding to 190-hHARE is required for HARE-mediated NF-κB-activated gene expression. Although we do not have a similar stable cell line expressing rHARE(ΔLink), previous studies showed that mAb-174, which was raised against rHARE, completely blocks HA uptake in stable cells expressing rHARE (29), in primary rat liver sinusoidal endothelial cells, and in intact perfused rat liver (30, 49). mAb-174 does not recognize hHARE. To test if HA binding to rHARE is required for NF-κB activation, we pre-blocked HA-binding sites in rHARE cells with mAb-174 and then treated with HA. Control treatment with mouse IgG had no effect on HA-stimulated gene expression. As expected, mAb-174 significantly blocked HA-HARE-mediated NF-κB activation ($p < 0.05$). Treatment with mouse IgG or mAb-174 alone (no HA) did not activate NF-κB signaling (Fig. 4*B*). These data confirm that HA

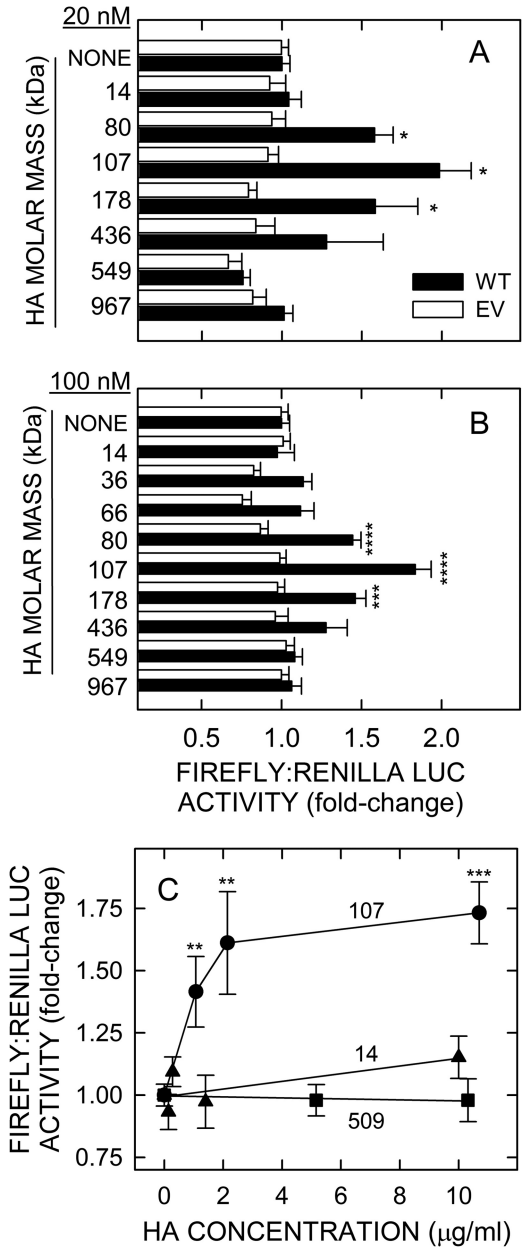

FIGURE 5. **HA size dependence for HARE-mediated NF-κB-activated gene expression.** EV (*white bars*) or hHARE (*black bars*) cells were incubated with 20 nM (*A*) or 100 nM (*B*) preparations of narrow size range HA of the indicated M_w values, representing sizes from the oHA-sHA boundary to high-range iHA, for 4 h, and then processed as in Fig. 3. *C,* dose-response curves expressed in weight concentration units (μg/ml) rather than molar units (nM) are shown using active 107 kDa and inactive 14- or 509-kDa HA preparations. Values for *p* comparing hHARE and EV cells ($n = 9$) are as follows: *, $p < 0.05$; **, $p < 0.005$; ***, $p < 0.001$; ****, $p < 0.0001$.

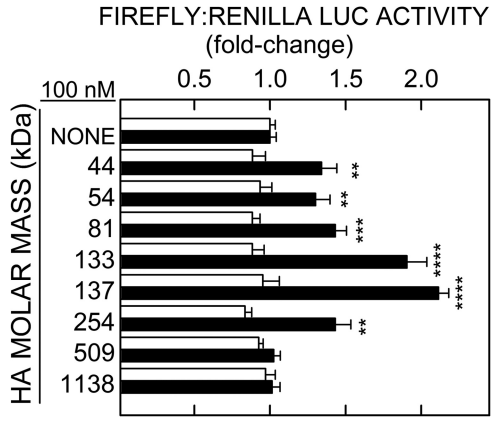

FIGURE 6. **Select-HA size dependence for HARE-mediated NF-κB-activated gene expression.** EV (*white bars*) or hHARE (*black bars*) cells were incubated with 100 nM of the indicated nearly monodisperse Select-HA for 4 h and processed as in Fig. 3. Values for *p* compare cell responses at each HA concentration ($n = 9$): **, $p < 0.005$; ***, $p < 0.001$; ****, $p < 0.0001$.

binding to rat or human HARE is required for NF-κB-activated gene expression.

Small to Intermediate HA but Not Smaller or Larger HA Stimulates HARE-mediated NF-κB Activation—To determine whether there is an HA size dependence for HARE-mediated NF-κB activation, we tested HA preparations with different size ranges from oHA-sHA to lHA (M_w: 14, 36, 66, 80, 107, 178, 436, 549, and 967 kDa) in both EV and hHARE cells. Interestingly, only mid-range to high-range sHA (M_w 80 kDa) and low-range iHA (M_w 107 and 178 kDa), but not mid-range to high-range iHA (M_w 436, 549, and 967 kDa) stimulated HARE-mediated NF-κB activation at both lower (20 nM; Fig. 5*A*, $p < 0.05$) and higher (100 nM; Fig. 5*B*, $p < 0.0001$) doses. The ability of different size HA preparations (at 100 nM) to stimulate NF-κB activation showed a bell-shaped curve overlapping high-range sHA and low-range iHA (*i.e.* spanning the boundary of 100 kDa). Using our "lab-made" narrow size range HA preparations, the peak response occurred at 107 kDa, and response intensity decreased with either increasing or decreasing HA size. Because the responses with 80- and 178-kDa HA were identical, we estimate that the optimal response size for HA is likely about 140 kDa. In contrast, EV cells showed no activation of NF-κB with any of the different HA size ranges tested at either 20 or 100 nM (Fig. 5, *A* and *B*). The same biphasic HA size dependence was observed in a dose-response experiment (Fig. 5*C*) using weight concentration values of small and large nonsignaling HA and 107-kDa signaling HA.

Select-HA™ Stimulates HARE-mediated NF-κB Activation—Because our purified narrow size range HA pools are still somewhat polydisperse (PD = 1.05–1.15), we tested essentially monodisperse (PD = 1.0–1.03) Select-HA from Hyalose, L.L.C. (50). To further define the optimum HA size for HARE-mediated NF-κB activation, we tested a broad range of M_w values from 44 to 1138 kDa (Fig. 6). As expected, the results confirmed that only small-intermediate size HA stimulated HARE-mediated NF-κB-activated gene expression, giving a bell-shaped curve with a peak that decreased with increasing or decreasing HA size. Mid-range iHA (509 kDa) or lHA (1,138 kDa) did not stimulate NF-κB activation.

Two additional features of the activation became evident when Select-HA rather than the narrow size range HA was used. First, rather than 107 kDa as found in Fig. 5, the optimal Select-HA size was 137 kDa, and the response would perhaps be even greater with slightly larger Select-HA. Using Select-HAs, the response with 137 kDa was significantly greater than with 107 kDa. Second, the ability to stimulate signaling was detected with smaller sizes ranging down to about 40 kDa. Apparently, the size heterogeneity of even the narrow size HA in this low mass range decreases the ability to detect activity of larger mol-

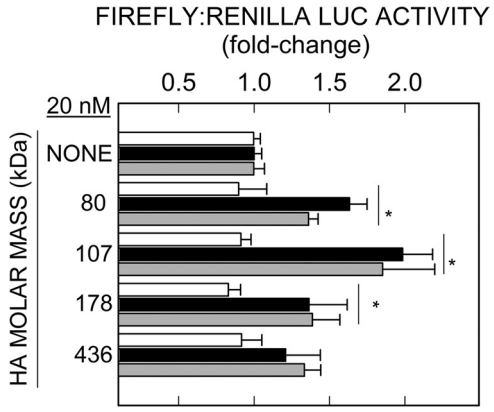

FIGURE 7. **Rat and human HARE show similar HA size dependence for NF-κB-activated gene expression.** EV (*white bars*), hHARE (*black bars*), or rHARE (*gray bars*) cells were incubated with 20 nM of different narrow size range HA preparations with the indicated M_w values for 4 h and processed as in Fig. 3. Values for *p* compare hHARE or rHARE with EV cells for each HA sample ($n = 6$): *, $p < 0.05$.

ecules (Figs. 2 and 5), whereas Select-HA of 44 and 54 kDa showed significant stimulations ($p < 0.005$). Nonetheless, using various preparations of oHA-sHA, sHA, iHA, and lHA, generated in our laboratory or obtained from Hyalose, we consistently observed that a relatively narrow range of small-intermediate HA (*i.e.* from mid-range sHA to mid-range iHA; 40–400 kDa) stimulated HARE- and NF-κB-mediated gene expression but that OHA, low-range sHA, mid-range, or high-range iHA and lHA did not stimulate this response.

Rat and Human HARE Show a Similar HA Size Dependence for NF-κB Activation—We then tested different HA size preparations for the ability to stimulate NF-κB activation in cells expressing rHARE (Fig. 7). There was no significant difference between rat and human HARE in the HA size dependence of NF-κB activation. Both receptor species mediated about a 2-fold stimulation of NF-κB activation with 107-kDa HA and showed decreasing activation with larger or smaller HA. The results indicate that mammalian HARE responds exclusively and very selectively to a narrow range of HA sizes, from ~40 to 400 kDa (*i.e.* from mid-range sHA to mid-range iHA; see the *dashed lines* in Fig. 1).

NF-κB Activation Stimulated by Low-range iHA Is Blocked by Large or Small HA—To assess possible competition for signaling by HA sizes outside the signaling range, we incubated hHARE or EV cells with 137-kDa Select-HA (a low-range iHA) with or without increasing doses of either a mid-range iHA, 509-kDa Select-HA (Fig. 8*A*), or a narrow range 14-kDa oHA (Fig. 8*B*). Both the larger and smaller HA blocked, in a dose-dependent manner, the ability of the signaling iHA to stimulate HARE-mediated NF-κB activation. NF-κB activation was not detected in EV cells treated with either HA species or in hHARE cells treated with the larger or smaller HA.

The above results indicate that not just the presence of an appropriate size HA, but the overall distribution and concentration of all HA sizes, to which HARE-expressing cells are exposed, will determine whether NF-κB activation occurs. In normal physiological samples, a broad range of HA sizes is normally present, including sHA, iHA, and lHA. To understand further the relevance of HARE-mediated NF-κB activation

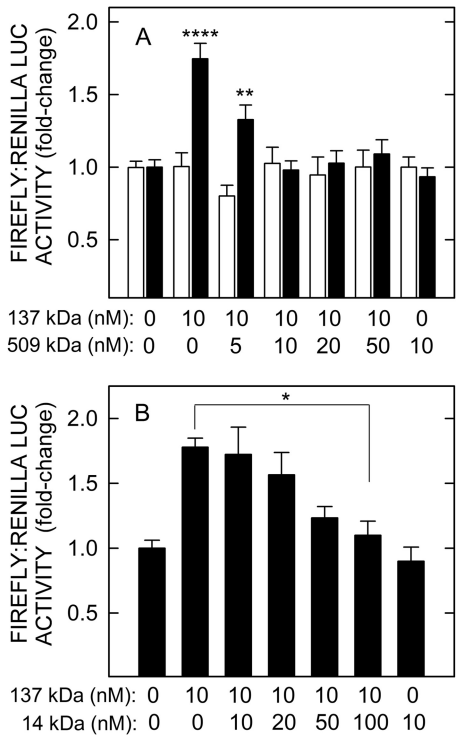

FIGURE 8. **Low-range iHA stimulation of HARE-mediated NF-κB activation is blocked by smaller or larger HA.** *A,* EV (*white bars*) and hHARE (*black bars*) cells were incubated with 137-kDa low range Select-iHA and the indicated concentrations of 509-kDa mid-range iHA for 4 h and processed as in Fig. 3. Values for *p* compared hHARE and EV cells at each HA concentration ($n = 9$) are as follows: **, $p < 0.005$; ****, $p < 0.0001$. *B,* hHARE cells were incubated with 137-kDa low-range Select-iHA and the indicated concentrations of narrow range 14-kDa oHA-iHA. *p* values compared 10 nM 137-kDa HA samples without *versus* with 14-kDa HA (*, $p < 0.05$; for 0 *versus* 100 nM: $n = 9$).

stimulated by a relatively narrow range of sHA and iHA, we tested 51- and 741-kDa polydisperse commercial HA preparations for their ability to signal (Fig. 9*A*). The 51-kDa, but not the 741-kDa, HA activated NF-κB, and when the two were mixed (1:1) the 51-kDa signaling response was reduced from ~2- to 1.3-fold. Although both preparations contained a broad range of sizes, ~55% of the 51-kDa HA was in the active range compared with 30% in the 741-kDa HA (*unshaded areas* in Fig. 9, *B* and *C*). Thus, the mixture has an ~0.43 fraction of active HA. The results demonstrate that HARE-mediated signaling occurs only above a threshold fraction of active HA in a given M_w sample.

Effect of sHA-iHA on the Degradation of IκB-α—IκB-α and IκB-β are endogenous proteins that inhibit NF-κB. In an inactive form, the p50 and p65 subunits of NF-κB form heteromeric complexes with the inhibitory IκB proteins and are sequestered in the cytoplasm. These inactive NF-κB complexes cannot translocate into the nucleus to interact with NF-κB promoters and regulate gene expression. The activation of NF-κB (*e.g.* by inflammatory cytokines such as TNF-α) is achieved through the phosphorylation of IκB-α at Ser^{32} and Ser^{36}, which targets the phosphoprotein for polyubiquitination and degradation (51). The degradation and decreased amount of the IκB inhibitor leads to the activation and nuclear translocation of NF-κB. To determine whether EV or hHARE cells used in this study are capable of activating this endogenous NF-κB pathway for gene expression, we assessed the effect of TNF-α, a strong positive

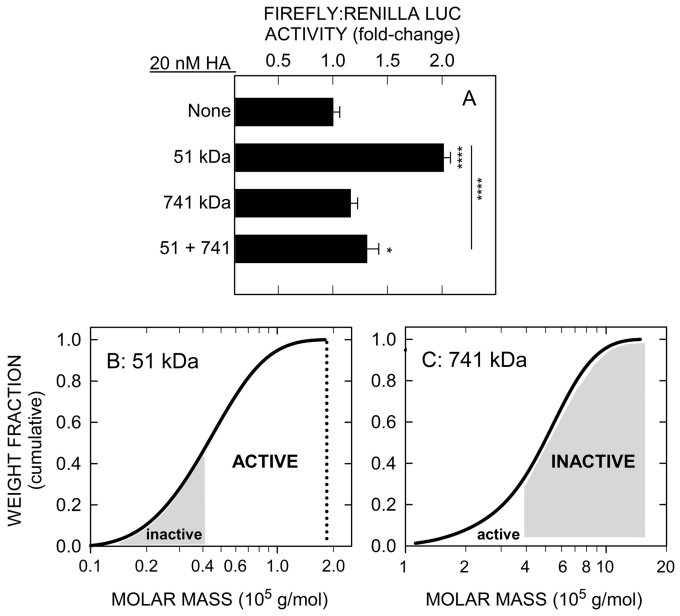

FIGURE 9. **HARE-mediated NF-κB activation by polydisperse HA occurs only if the active HA size fraction is high enough.** *A,* cells expressing hHARE were incubated with medium alone (no addition) or 20 nM of polydisperse 51 or 741 kDa or 40 nM of a 1:1 mixture and processed as in Fig. 3. Significant differences are indicated by a symbol above a bar (left of line) for comparison with the no addition sample or by a symbol to the right of the line for comparison with the 51-kDa sample (*, $p < 0.05$; ****, $p < 0.0001$; $n = 9$). SEC-MALLS analysis of the cumulative weight fractions of 51-kDa (*B*) and 741-kDa (*C*) HA reveals that the fraction of active HA in the 40–400-kDa range (*unshaded area*) is greater than the inactive fraction (*gray shaded area*) in the 51-kDa but not in the 741-kDa HA preparations.

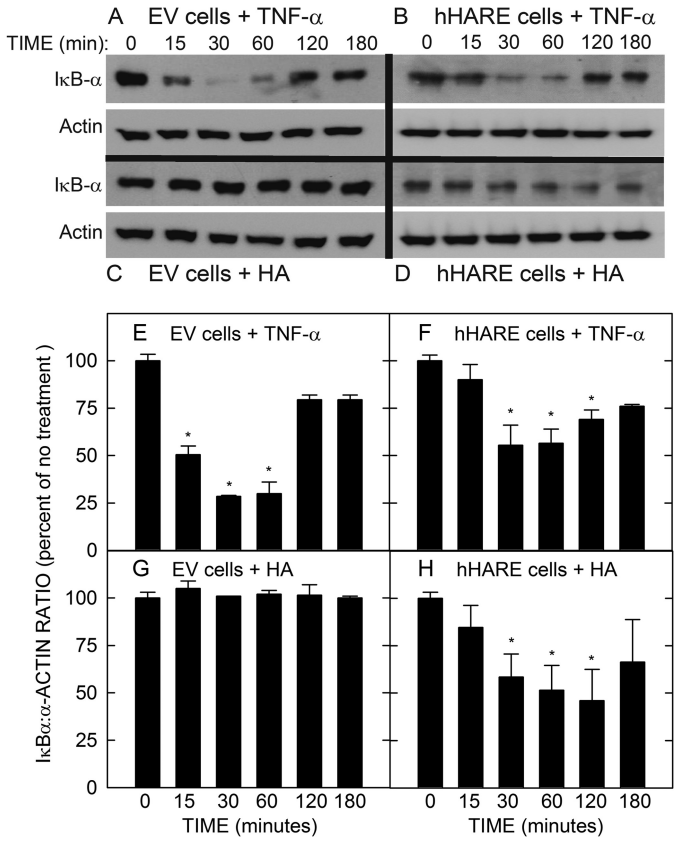

FIGURE 10. **Effect of TNF-α and HA on IκB-α degradation.** EV (*A, C, E,* and *G*) or hHARE (*B, D, F,* and *H*) cells were grown to confluence and washed. After a 1-h serum-free medium incubation at 37 °C, the cells were incubated with 1 ng/ml TNF-α (*A, B, E,* and *F*) or 100 nM 137-kDa HA (*C, D, G,* and *H*) for 0–180 min as indicated. Cells were processed and Western blot analyses performed with a mAb against IκB-α (*A–D, top of panels*) as under "Experimental Procedures." The same membranes were stripped and reprobed with anti-actin Ab as an internal loading control (*A–D, bottom of panels*). Blots from three independent experiments were digitized by scanning, and densitometric analysis was performed to determine the IκB-α/α-actin ratios at each time. Normalized data (*E–H*) are presented as mean ± S.E. ($n = 3$) percent of the IκB-α/α-actin ratio relative to the no addition time 0 value as 100% (*E–H*); *, $p < 0.05$.

activator of NF-κB, on IκB-α degradation. After TNF-α treatment, significant decreases in IκB-α levels (45–65%) were observed by 30–60 min in both cell types (Fig. 10, *A*, *B*, *E,* and *F*). By 2 and 3 h, IκB-α protein levels were recovering and increased to ~75% of the initial value. Thus, EV and hHARE cell lines showed an expected intracellular activation of NF-κB due to degradation of IκB-α after stimulation with TNF-α.

To confirm that small-intermediate size HA indeed stimulates an endogenous HARE-mediated NF-κB pathway in the absence of the Dual-Luciferase reporter system, hHARE and EV cells were incubated with 137-kDa HA for various times, and IκB-α levels were assessed as above. HA treatment of EV cells had no effect on the amount of IκB-α (Fig. 10, *C* and *G*). In contrast, the level of IκB-α in treated hHARE cells dropped significantly ($p < 0.05$) from 30 to 120 min, reaching a maximum 55% decrease at 120 min (Fig. 10, *D* and *H*). By 3 h, the IκB-α level in HA-treated cells had begun to rebound, increasing to ~65% of control. Treatment with TNF-α or HA did not alter the levels of actin, an unrelated control protein, in the same cells (Fig. 10, *A–D*). These results confirm that sHA-iHA stimulates HARE-mediated cell signaling via endogenous activation of NF-κB pathways and thus corroborates the use of the NF-κB promoter-driven luciferase gene expression assays to quantify the signaling responses.

Small but Not Large HA Stimulates HARE-mediated ERK Phosphorylation in a Time-dependent Manner—We previously found that HA binding to the Link domain is required for HA-HARE-mediated ERK1/2 activation (31), but we did not examine the HA size dependence for HARE-mediated signaling. To assess this, we incubated EV or hHARE cells with an sHA (80 kDa) preparation that activated NF-κB-mediated gene expression or an iHA (560 kDa) preparation that was inactive (Fig. 11). Cell extracts were processed for Western analyses to detect ERK1/2 activation as described previously (31). As expected, neither HA size had any effect on ERK1/2 activation in EV cells (Fig. 11, *A* and *C*). Cells expressing HARE showed no activation of ERK1/2 by the 560-kDa IHA (Fig. 11*B*), but the 80-kDa sHA stimulated significant phosphorylation of ERK1/2 in a time-dependent manner (Fig. 11*D*). hHARE cells treated with the sHA for 15 min showed a 2.3-fold increase in pERK1/2 ($p < 0.001$); the response decreased by 30 min to a 1.8-fold increase that was still significantly elevated ($p < 0.005$). Thus, the previously identified HA- and HARE-dependent ERK1/2 activation shows a similar HA size dependence to that for the activation of NF-κB-mediated gene expression.

Many questions remain unanswered, including whether HA endocytosis is required for HARE-mediated cell signaling and whether NF-κB and ERK activations are linked. However, it was not possible to use specific agents such as dynasore or MEK inhibitors, because TNF-α-induced (supplemental Fig. S4*A*)

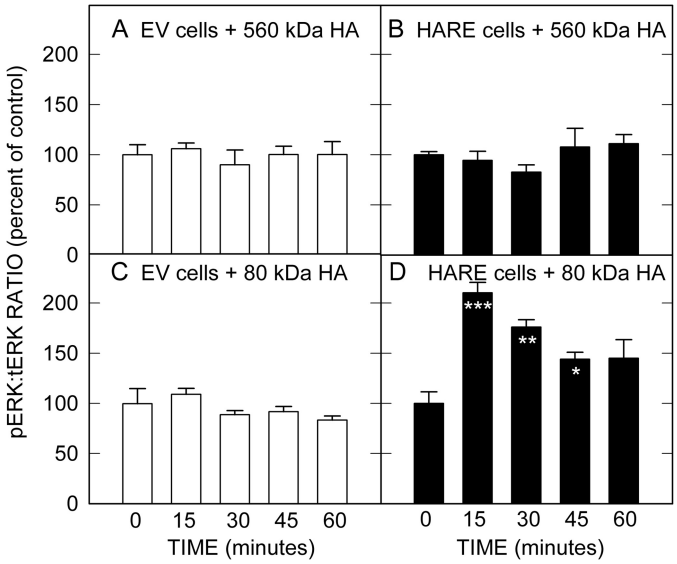

FIGURE 11. **HARE-mediated ERK activation also shows HA size dependence.** EV (*A* and *C*) or hHARE (*B* and *D*) cells were grown to confluence, washed, incubated in serum-free medium at 37 °C for 1 h, and then incubated with or without 10 μg/ml 80-kDa (*A* and *B*) or 560-kDa (*C* and *D*) HA for the indicated times. Lysate samples were subjected to 10% SDS-PAGE and Western analysis with Ab against phospho-ERK1/2 (*pERK1/2*) and then, after stripping, with Ab against total ERK1/2 protein (*tERK1/2*) and anti-actin (31). Blots from three to four independent experiments were digitized, and densitometric analysis was performed to determine the phospho-ERK/total ERK ratios at each time. Values are the mean ± S.E. ($n = 3–4$) percent of the phospho-ERK/total ERK ratio relative to time 0 (the no addition value) as 100%. *p* values compare the sample pairs at time 0 and the indicated time (*, $p < 0.05$; **, $p < 0.005$; ***, $p < 0.001$).

and HA-induced (supplemental Fig. S4*B*) NF-κB activations were both blocked by DMSO; results similar to the DMSO inhibition of HA fragment induced NF-κB activation of inflammatory gene expression in mouse alveolar macrophage and epithelial cells (52).

DISCUSSION

For this study we used non-animal-derived low endotoxin HA preparations, either commercial polydisperse and Select-HA or narrow size range preparations of HA purified by SEC fractionation and parallel SEC-MALLS analysis. SEC-MALLS is one of the most accurate methods to characterize an HA sample by simultaneously measuring multiple parameters that enable determination of number-average and weight-average molar masses, polymer size distribution, polydispersity, and concentration. The laboratory-made preparations (Fig. 5) indicated a maximum signaling response with 107-kDa HA and an active size range between about 36 and 436 kDa (M_w). The Select-HAs, which are as close to monodisperse as any HA available (53), revealed a maximum response with 137 kDa and an active size range of at least 44–254 kDa (Fig. 6). Based on the Select-HA results and the narrow range HA responses, we estimate that the optimal HA size for signaling is likely between 140 and 150 kDa, and the active fragment size range is between 40 and 400 kDa. In more complex physiological situations with polydisperse HA that has a broad size range, signaling will only occur if the fraction of HA in the active size range is high enough to offset the effect of competition by the inactive smaller and larger HA fractions (Fig. 9).

We note our use of molar concentration units, rather than weight concentrations, because it is more appropriate when comparing HA preparations of different M_w and also enables an easier comparison with receptor-ligand binding parameters. If weight concentration values are used, the same biphasic HA size dependence is observed (Fig. 5*C*). HA-HARE-mediated stimulation of NF-κB activation was dose-dependent with an apparent K_m value of ~10 nM, which is nearly identical (25, 27) to the dissociation constant for HA-HARE complexes in cells expressing recombinant hHARE (K_d ~7 nM) or purified ectodomain (K_d ~10–20 nM).

HARE is a constitutively recycling receptor that functions in the same way as the LDL and asialoglycoprotein receptors (54–56). These receptors continuously traverse a spatial and temporal pathway in which they are internalized from the surface via coated pits, whether ligand is bound or not, travel through a series of intracellular compartments (during which bound ligand is dissociated and delivered to lysosomes), and then return to the plasma membrane, ready for another cycle. Receptor recycling times are 8–12 min. Because ligand binding is not needed for receptor internalization, bound ligands are co-endocytosed as cargo. Therefore, HA of any size able to bind HARE will be internalized.

Laurent and Fraser (4) discovered the receptor using metabolically labeled MDa [^{3}H]HA. We have used higher specific activity 50–150 kDa ^{125}I-HA, uniquely modified at the reducing end (56, 57). To examine the oHA size range for HARE binding, we assessed the ability of [^{3}H]HA oligomers, 10–20 sugars long, to bind purified 190-hHARE ectodomain in a ligand blot-autoradiography format (supplemental Fig. S5*A*). Binding to HARE occurred with all six oligosaccharides tested but increased 35-fold with increasing size (supplemental Fig. S5*B*). Thus, the sizes of HA that are able to bind and be endocytosed by HARE range from 8 to 50,000 sugars (<2 kDa to 10 MDa). Any HA molecule able to span a Link domain-binding site (≥ 8 sugars) can bind HARE and be internalized.

The 35-fold binding increase as oHA length increased from 10 to 20 sugars (supplemental Fig. S5*B*) is consistent with the expected higher affinity and lower K_d values as HA size increases. This phenomenon was first reported for this receptor by Laurent *et al.* (58), who found that the K_d varied from 4.6 μM (4,600 nM) for an 8-mer to 9 pM (0.009 nM) for 6 MDa HA. The HA binding affinity for any HA-binding protein depends on the HA size used. Higher affinity is the biochemical consequence of greater multivalency proportional to increasing HA size. This is evident in Fig. 8 by the different competitive effectiveness of 14-*versus* 509-kDa HA, expressed on a molar basis. The larger HA is far more effective at low doses because it has more HA-binding sites per molecule than the 14-kDa HA.

The molecular basis for the narrow size dependence for HA signaling is unknown, but several scenarios could explain why oHA or lHA binding to HARE is not able, but sHA-iHA is able, to organize HARE in appropriately configured complexes (at the plasma membrane, in early endosomes, or both) to induce downstream cell signaling cascades. We favor a model in which the optimum length for an HA fragment is one that binds multiple HARE proteins and brings them in close enough proximity for the HA-induced oligomeric cytoplasmic domains to inter-

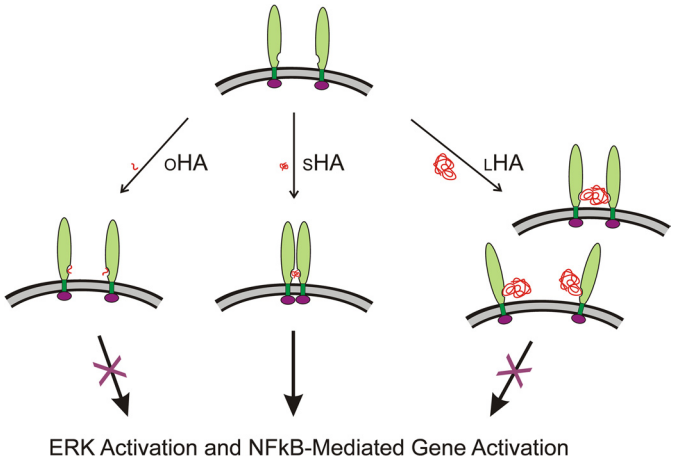

FIGURE 12. **Model for the HA size dependence of HARE-mediated cell signaling.** The scheme shows several possibilities for how two HARE proteins are able to interact with and bind to the same HA molecule, depending on the mass, and thus length, of the HA. Signaling does not occur with oHA or sHA <40 kDa because HA of this size is only able to bind one HARE protein (*left*). Signaling HA, between 40 and 400 kDa, is long enough to bind to two HARE molecules and yet short enough that the two proteins are brought into close proximity, inducing their cytoplasmic domains to interact and create complexes with signaling molecules (*middle*). Two proteins are shown, but three, four, or more HARE molecules could interact in a similar HA size-dependent manner to achieve cytoplasmic domain signaling complexes (*e.g.* trimers or tetramers). Complexes could occur in which two or more HARE proteins bind with the same HA to create dimers, dimers of dimers (tetramers), or a larger closed circular complex in which >4 cytoplasmic domains are brought together. As HA length increases, the bound HARE proteins are more likely to be further apart and not interact (*right*), even though more than two receptors may bind to the same HA; monomeric HA-HARE complexes may also occur.

act and present new interfaces for binding and activating signaling molecules (Fig. 12). HA smaller than a critical mass (length) cannot simultaneously bind and keep in close proximity multiple receptors, and therefore this HA size creates HA-HARE monomers. Larger HA than this critical mass can bind to two or more receptors, but with increasing probability that as HA size increases the receptor cytoplasmic domains will be too far apart to create a functional oligomer capable of intracellular signaling. It is inherent in the model that the affinity of HARE-HARE interactions (via cytoplasmic, ecto-, or membrane domains) increases when HA is bound. Models in which HARE proteins are bound in an open linear chain do not explain the HA size dependence.

Our results indicate that the relative concentrations and ratio of signaling HA to nonsignaling HA will determine the extent of HA-HARE-mediated cell signaling leading to NF-κB-activated gene expression. Native lHA in various tissues (typically M_w = 2–7 MDa) is considered anti-inflammatory and protective and has been used clinically to decrease inflammation joint and lung diseases (59, 60) and noninfectious lung injury (12, 43). As noted in the Introduction, many reports in various cell types and animal models have documented different biological effects of HA based on its size. In addition to HARE, the HA receptors CD44 and RHAAM also signal in response to smaller but not larger HA (62, 63). Small HA fragments are thought to occur at inflammation sites and be active in inducing expression of inflammatory genes, such as TNF-α, IL-1β (64).

It is more technically challenging to detect and quantify small *versus* large HA, and few studies have determined the endogenous tissue levels of various HA size ranges in normal or pathological situations. Similarly, few reports have studied both HA size and levels in the serum of healthy people or during pathological situations. The serum HA level in healthy people is 25 ng/ml and the size is ~100-kDa HA (34, 65). Reticulum cell sarcoma and neuroblastoma patients showed abundant sHA (~58 kDa) in serum, which was not detected in healthy people (66). SEC analysis of serum HA from healthy donors and patients with rheumatoid arthritis or primary biliary cirrhosis revealed varied concentrations of low-range iHA (140–270 kDa). Healthy donors had a relatively low serum HA concentration (21 μg/liter), whereas rheumatoid arthritis (397 μg/liter) and biliary cirrhosis (629 μg/liter) patients showed highly increased levels (67). All the HA sizes reported in the above studies are within the signaling size range for HA activation of HARE-mediated signaling in sinusoidal endothelial cells of liver and perhaps spleen.

HARE and Stab2 are constitutively recycling receptors (25, 56) that bind and internalize, via clathrin-mediated endocytosis, 14 different ligands that represent tissue ECM degradation products or dead cell debris (25, 32, 68). Our earlier finding that HA-HARE complexes activate ERK1/2 (31) indicates that the function of HARE is not just the clearance of HA, leading to its degradation. The present findings that HARE-mediated activation of ERK1/2 and NF-κB-mediated gene expression occur within a narrow size range of HA products supports a recently proposed Tissue Stress Sensor hypothesis (42) that the HARE clearance system functions to monitor the health and homeostasis of tissues throughout the body. Cellular and ECM tissue components normally turnover as they are continuously synthesized and degraded at characteristic rates (*i.e.* defining their biological half-lives). The HARE/Stab2 signaling system may respond to an endogenous danger signal (*e.g.* abnormally high levels of circulating degraded HA) indicating a tissue stress situation (*e.g.* due to injury, infection, inflammation, oxidative damage, or other stress) that creates a homeostasis imbalance in tissue matrix turnover, as reflected in increased levels of tissue matrix breakdown products. Ongoing studies indicate that, in addition to HA, some of the other glycosaminoglycan and nonglycosaminoglycan HARE ligands are also able to activate NF-κB-mediated gene expression.[3] Thus, the HARE signaling system may respond to multiple circulating systemic ECM degradation and tissue stress-indicator ligands, whose relative concentrations and ratios reflect the turnover and damage status of tissues throughout the body. Preliminary studies also indicate that signaling by HA, but not other ligands, is lost by elimination of the HARE Link domain *N*-glycan (61).

In summary, our results show that HA-HARE interactions stimulate NF-κB activation of gene expression and support a previous finding that HA binding to HARE can activate ERK1/2, which shows a similar dependence on HA size. The receptor sensing system for HA size detects and responds to a narrow size range of HA degradation products (40–400 kDa). This active signaling HA size range corresponds to the circulating HA size range reported for healthy people and those with

[3] M. S. Pandey and P. H. Weigel, unpublished results.

various diseases. Thus, this HARE receptor signaling system operating in parallel with its HA clearance function could play an important role in monitoring the status of issue biomatrix turnover and stress throughout the body.

Acknowledgments—We thank Dr. K. Mark Coggeshall, Dr. Paul DeAngelis, Dr. Ann L. Olson, and Dr. Arjun Thapa for reagents and helpful discussions.

REFERENCES

1. Laurent, T. C., Laurent, U. B., and Fraser, J. R. (1996) The structure and function of hyaluronan: An overview. *Immunol. Cell Biol.* **74,** A1–A7
2. Toole, B. P. (1990) Hyaluronan and its binding proteins, the hyaladherins. *Curr. Opin. Cell Biol.* **2,** 839–844
3. Day, A. J., and Prestwich, G. D. (2002) Hyaluronan-binding proteins: tying up the giant. *J. Biol. Chem.* **277,** 4585–4588
4. Laurent, T. C., and Fraser, J. R. (1992) Hyaluronan. *FASEB J.* **6,** 2397–2404
5. Knudson, C. B., and Knudson, W. (1993) Hyaluronan-binding proteins in development, tissue homeostasis, and disease. *FASEB J.* **7,** 1233–1241
6. Toole, B. P. (1997) Hyaluronan in morphogenesis. *J. Intern. Med.* **242,** 35–40
7. Abatangelo, G., and Weigel, P. H. (eds (2000) *Redefining Hyaluronan*. Elsevier Science Publishers B.V., Amsterdam
8. Stern, R., Asari, A. A., and Sugahara, K. N. (2006) Hyaluronan fragments: an information-rich system. *Eur. J. Cell Biol.* **85,** 699–715
9. Termeer, C., Sleeman, J. P., and Simon, J. C. (2003) Hyaluronan–magic glue for the regulation of the immune response? *Trends Immunol.* **24,** 112–114
10. Anttila, M. A., Tammi, R. H., Tammi, M. I., Syrjänen, K. J., Saarikoski, S. V., and Kosma, V. M. (2000) High levels of stromal hyaluronan predict poor disease outcome in epithelial ovarian cancer. *Cancer Res.* **60,** 150–155
11. Hascall, V. C., Majors, A. K., De La Motte, C. A., Evanko, S. P., Wang, A., Drazba, J. A., Strong, S. A., and Wight, T. N. (2004) Intracellular hyaluronan: a new frontier for inflammation? *Biochim. Biophys. Acta* **1673,** 3–12
12. Noble, P. W. (2002) Hyaluronan and its catabolic products in tissue injury and repair. *Matrix Biol.* **21,** 25–29
13. Mapp, P. I., Grootveld, M. C., and Blake, D. R. (1995) Hypoxia, oxidative stress, and rheumatoid arthritis. *Br. Med. Bull.* **51,** 419–436
14. Sampson, P. M., Rochester, C. L., Freundlich, B., and Elias, J. A. (1992) Cytokine regulation of human lung fibroblast hyaluronan (hyaluronic acid) production. Evidence for cytokine-regulated hyaluronan (hyaluronic acid) degradation and human lung fibroblast-derived hyaluronidase. *J. Clin. Invest.* **90,** 1492–1503
15. Estes, J. M., Adzick, N. S., Harrison, M. R., Longaker, M. T., and Stern, R. (1993) Hyaluronate metabolism undergoes an ontogenic transition during fetal development: implications for scar-free wound healing. *J. Pediatr. Surg.* **28,** 1227–1231
16. Khaing, Z. Z., Milman, B. D., Vanscoy, J. E., Seidlits, S. K., Grill, R. J., and Schmidt, C. E. (2011) High molecular weight hyaluronic acid limits astrocyte activation and scar formation after spinal cord injury. *J. Neural Eng.* **8,** 046033
17. Deed, R., Rooney, P., Kumar, P., Norton, J. D., Smith, J., Freemont, A. J., and Kumar, S. (1997) Early-response gene signalling is induced by angiogenic oligosaccharides of hyaluronan in endothelial cells. Inhibition by non-angiogenic, high-molecular-weight hyaluronan. *Int. J. Cancer* **71,** 251–256
18. West, D. C., Hampson, I. N., Arnold, F., and Kumar, S. (1985) Angiogenesis induced by degradation products of hyaluronic acid. *Science* **228,** 1324–1326
19. Kim, K. W., Cho, M. L., Lee, S. H., Oh, H. J., Kang, C. M., Ju, J. H., Min, S. Y., Cho, Y. G., Park, S. H., and Kim, H. Y. (2007) Human rheumatoid synovial fibroblasts promote osteoclastogenic activity by activating RANKL via TLR-2 and TLR-4 activation. *Immunol. Lett.* **110,** 54–64
20. Kumar, A., Takada, Y., Boriek, A. M., and Aggarwal, B. B. (2004) Nuclear factor-κB: its role in health and disease. *J. Mol. Med.* **82,** 434–448
21. Karin, M., and Ben-Neriah, Y. (2000) Phosphorylation meets ubiquitination: the control of NF-κB activity. *Annu. Rev. Immunol.* **18,** 621–663
22. Ghosh, S., May, M. J., and Kopp, E. B. (1998) NF-κB and Rel proteins: evolutionarily conserved mediators of immune responses. *Annu. Rev. Immunol.* **16,** 225–260
23. Fujii, K., Tanaka, Y., Hübscher, S., Saito, K., Ota, T., and Eto, S. (1999) Crosslinking of CD44 on rheumatoid synovial cells augment interleukin 6 production. *Lab. Invest.* **79,** 1439–1446
24. Fieber, C., Baumann, P., Vallon, R., Termeer, C., Simon, J. C., Hofmann, M., Angel, P., Herrlich, P., and Sleeman, J. P. (2004) Hyaluronan-oligosaccharide-induced transcription of metalloproteases. *J. Cell Sci.* **117,** 359–367
25. Harris, E. N., Weigel, J. A., and Weigel, P. H. (2004) Endocytic function, glycosaminoglycan specificity, and antibody sensitivity of the recombinant human 190-kDa hyaluronan receptor for endocytosis (HARE). *J. Biol. Chem.* **279,** 36201–36209
26. Zhou, B., Weigel, J. A., Fauss, L., and Weigel, P. H. (2000) Identification of the hyaluronan receptor for endocytosis (HARE). *J. Biol. Chem.* **275,** 37733–37741
27. Harris, E. N., Kyosseva, S. V., Weigel, J. A., and Weigel, P. H. (2007) Expression, processing, and glycosaminoglycan binding activity of the recombinant human 315-kDa hyaluronic acid receptor for endocytosis (HARE). *J. Biol. Chem.* **282,** 2785–2797
28. Zhou, B., McGary, C. T., Weigel, J. A., Saxena, A., and Weigel, P. H. (2003) Purification and molecular identification of the human hyaluronan receptor for endocytosis. *Glycobiology* **13,** 339–349
29. Zhou, B., Weigel, J. A., Saxena, A., and Weigel, P. H. (2002) Molecular cloning and functional expression of the rat 175-kDa hyaluronan receptor for endocytosis. *Mol. Biol. Cell* **13,** 2853–2868
30. Zhou, B., Oka, J. A., Singh, A., and Weigel, P. H. (1999) Purification and subunit characterization of the rat liver endocytic hyaluronan receptor. *J. Biol. Chem.* **274,** 33831–33834
31. Kyosseva, S. V., Harris, E. N., and Weigel, P. H. (2008) The hyaluronan receptor for endocytosis mediates hyaluronan-dependent signal transduction via extracellular signal-regulated kinases. *J. Biol. Chem.* **283,** 15047–15055
32. Park, S. Y., Jung, M. Y., Kim, H. J., Lee, S. J., Kim, S. Y., Lee, B. H., Kwon, T. H., Park, R. W., and Kim, I. S. (2008) Rapid cell corpse clearance by stabilin-2, a membrane phosphatidylserine receptor. *Cell Death Differ.* **15,** 192–201
33. Lebel, L., Gabrielsson, J., Laurent, T. C., and Gerdin, B. (1994) Kinetics of circulating hyaluronan in humans. 4. *Eur. J. Clin. Invest.* **24,** 621–626
34. Laurent, T. C., and Fraser, J. R. (1991) in *Degradation of Bioactive Substances: Physiology and Pathophysiology* (Henriksen, J. H., ed) pp. 249–265, CRC Press, Inc., Boca Raton, FL
35. Fraser, J. R., Laurent, T. C., Pertoft, H., and Baxter, E. (1981) Plasma clearance, tissue distribution, and metabolism of hyaluronic acid injected intravenously in the rabbit. *Biochem. J.* **200,** 415–424
36. Qian, H., Johansson, S., McCourt, P., Smedsrød, B., Ekblom, M., and Johansson, S. (2009) Stabilins are expressed in bone marrow sinusoidal endothelial cells and mediate scavenging and cell adhesive functions. *Biochem. Biophys. Res. Commun.* **390,** 883–886
37. Falkowski, M., Schledzewski, K., Hansen, B., and Goerdt, S. (2003) Expression of stabilin-2, a novel fasciclin-like hyaluronan receptor protein, in murine sinusoidal endothelia, avascular tissues, and at solid/liquid interfaces. *Histochem. Cell Biol.* **120,** 361–369
38. Pandey, M. S., Harris, E. N., Weigel, J. A., and Weigel, P. H. (2008) The cytoplasmic domain of the hyaluronan receptor for endocytosis (HARE) contains multiple endocytic motifs targeting coated pit-mediated internalization. *J. Biol. Chem.* **283,** 21453–21461
39. Bradford, M. M. (1976) A rapid and sensitive method for the quantitation of microgram quantities of protein utilizing the principle of protein-dye binding. *Anal. Biochem.* **72,** 248–254
40. Baggenstoss, B. A., and Weigel, P. H. (2006) Size exclusion chromatography-multiangle laser light scattering analysis of hyaluronan size distributions made by membrane-bound hyaluronan synthase. *Anal. Biochem.* **352,** 243–251
41. Lee, H. G., and Cowman, M. K. (1994) An agarose gel electrophoretic

method for analysis of hyaluronan molecular weight distribution. *Anal. Biochem.* **219,** 278–287
42. Weigel, P. H., Pandey, M. S., and Harris, E. N. (2012) in *Structure and Function of Biomatrix: Control of Cell Function and Gene Expression* (Balazs, E. A., ed) pp. 293–314, Matrix Biology Institute, Edgewater, NJ
43. Jiang, D., Liang, J., and Noble, P. W. (2007) Hyaluronan in tissue injury and repair. *Annu. Rev. Cell Dev. Biol.* **23,** 435–461
44. Weigel, P. H., and Baggenstoss, B. A. (2012) Hyaluronan synthase polymerizing activity and control of product size are discrete enzyme functions that can be uncoupled by mutagenesis of conserved cysteines. *Glycobiology* **22,** 1302–1310
45. Bollyky, P. L., Lord, J. D., Masewicz, S. A., Evanko, S. P., Buckner, J. H., Wight, T. N., and Nepom, G. T. (2007) Cutting edge: high molecular weight hyaluronan promotes the suppressive effects of $CD4^+CD25^+$ regulatory T cells. *J. Immunol.* **179,** 744–747
46. Nakamura, K., Yokohama, S., Yoneda, M., Okamoto, S., Tamaki, Y., Ito, T., Okada, M., Aso, K., and Makino, I. (2004) High, but not low, molecular weight hyaluronan prevents T-cell-mediated liver injury by reducing proinflammatory cytokines in mice. *J. Gastroenterol.* **39,** 346–354
47. Scheibner, K. A., Lutz, M. A., Boodoo, S., Fenton, M. J., Powell, J. D., and Horton, M. R. (2006) Hyaluronan fragments act as an endogenous danger signal by engaging TLR2. *J. Immunol.* **177,** 1272–1281
48. Bronstein, I., Fortin, J., Stanley, P. E., Stewart, G. S., and Kricka, L. J. (1994) Chemiluminescent and bioluminescent reporter gene assays. *Anal. Biochem.* **219,** 169–181
49. Weigel, J. A., Raymond, R. C., McGary, C., Singh, A., and Weigel, P. H. (2003) A blocking antibody to the hyaluronan receptor for endocytosis (HARE) inhibits hyaluronan clearance by perfused liver. *J. Biol. Chem.* **278,** 9808–9812
50. Jing, W., and DeAngelis, P. L. (2004) Synchronized chemoenzymatic synthesis of monodisperse hyaluronan polymers. *J. Biol. Chem.* **279,** 42345–42349
51. Senftleben, U., and Karin, M. (2002) The IKK/NF-κ pathway. *Crit. Care Med.* **30,** S18-S26
52. Eberlein, M., Scheibner, K. A., Black, K. E., Collins, S. L., Chan-Li, Y., Powell, J. D., and Horton, M. R. (2008) *J. Inflamm.* **5,** 20
53. DeAngelis, P. L. (2008) Monodisperse hyaluronan polymers: synthesis and potential applications. *Curr. Pharm. Biotechnol.* **9,** 246–248
54. Weigel, P. H., and Yik, J. H. (2002) Glycans as endocytosis signals: the cases of the asialoglycoprotein and hyaluronan/chondroitin sulfate receptors. *Biochim. Biophys. Acta* **1572,** 341–363
55. Goldstein, J. L., and Brown, M. S. (2009) The LDL receptor. *Arterioscler. Thromb. Vasc. Biol.* **29,** 431–438
56. McGary, C. T., Raja, R. H., and Weigel, P. H. (1989) Endocytosis of hyaluronic acid by rat liver endothelial cells. Evidence for receptor recycling. *Biochem. J.* **257,** 875–884
57. Raja, R. H., LeBoeuf, R. D., Stone, G. W., and Weigel, P. H. (1984) Preparation of alkylamine and ^{125}I-radiolabeled derivatives of hyaluronic acid uniquely modified at the reducing end. *Anal. Biochem.* **139,** 168–177
58. Laurent, T. C., Fraser, J. R., Pertoft, H., and Smedsrød, B. (1986) Binding of hyaluronate and chondroitin sulphate to liver endothelial cells. *Biochem. J.* **234,** 653–658
59. Goto, M., Hanyu, T., Yoshio, T., Matsuno, H., Shimizu, M., Murata, N., Shiozawa, S., Matsubara, T., Yamana, S., and Matsuda, T. (2001) Intra-articular injection of hyaluronate (SI-6601D) improves joint pain and synovial fluid prostaglandin E2 levels in rheumatoid arthritis: a multicenter clinical trial. *Clin. Exp. Rheumatol.* **19,** 377–383
60. Cantor, J. O., Cerreta, J. M., Keller, S., and Turino, G. M. (1995) Modulation of airspace enlargement in elastase-induced emphysema by intratracheal instillment of hyaluronidase and hyaluronic acid. *Exp. Lung Res.* **21,** 423–436
61. Harris, E. N., Parry, S., Sutton-Smith, M., Pandey, M. S., Panico, M., Morris, H. R., Haslam, S. M., Dell, A., and Weigel, P. H. (2010) *N*-Glycans on the link domain of human HARE/Stabilin-2 are needed for hyaluronan binding to purified ectodomain, but not for cellular endocytosis of hyaluronan. *Glycobiology* **20,** 991–1001
62. Bourguignon, L. Y., Wong, G., Earle, C. A., and Xia, W. (2011) Interaction of low molecular weight hyaluronan with CD44 and toll-like receptors promotes the actin filament-associated protein 110-actin binding and MyD88-NFκB signaling leading to proinflammatory cytokine/chemokine production and breast tumor invasion. *Cytoskeleton* **68,** 671–693
63. Kouvidi, K., Berdiaki, A., Nikitovic, D., Katonis, P., Afratis, N., Hascall, V. C., Karamanos, N. K., and Tzanakakis, G. N. (2011) Role of receptor for hyaluronic acid-mediated motility (RHAMM) in low molecular weight hyaluronan (LMWHA)-mediated fibrosarcoma cell adhesion. *J. Biol. Chem.* **286,** 38509–38520
64. Adair-Kirk, T. L., and Senior, R. M. (2008) Fragments of extracellular matrix as mediators of inflammation. *Int. J. Biochem. Cell Biol.* **40,** 1101–1110
65. Elliott, A. L., Kraus, V. B., Luta, G., Stabler, T., Renner, J. B., Woodard, J., Dragomir, A. D., Helmick, C. G., Hochberg, M. C., and Jordan, J. M. (2005) Serum hyaluronan levels and radiographic knee and hip osteoarthritis in African Americans and Caucasians in the Johnston County Osteoarthritis Project. *Arthritis Rheum.* **52,** 105–111
66. Deutsch, H. F. (1957) Some properties of a human serum hyaluronic acid. *J. Biol. Chem.* **224,** 767–774
67. Tengblad, A., Laurent, U. B., Lilja, K., Cahill, R. N., Engström-Laurent, A., Fraser, J. R., Hansson, H. E., and Laurent, T. C. (1986) Concentration and relative molecular mass of hyaluronate in lymph and blood. *Biochem. J.* **236,** 521–525
68. Smedsrød, B., Malmgren, M., Ericsson, J., and Laurent, T. C. (1988) Morphological studies on endocytosis of chondroitin sulphate proteoglycan by rat liver endothelial cells. *Cell Tissue Res.* **253,** 39–45

SUPPLEMENTARY FIGURE LEGENDS

Figure S1. Time-dependence for HARE-mediated NF-κB gene expression activated by sHA in hHARE cells. Cells expressing hHARE were transfected for 18 h, washed and incubated in serum-free medium for 1 h, washed and incubated with 125 nM (10 μg/ml) 80 kDa HA for 4 h and processed to determine LUC activities as described in Fig. 3 and *Experimental Procedures*. Values are the mean ± SE (n=3) firefly:Renilla LUC ratio expressed as a percent of the time-zero, no addition control; ***, $p < 0.001$.

Figure S2. TNF-α activates NF-κB in a dose-dependent manner in Flp-In 293 cells. Cells expressing hHARE (black) or EV (white) were transiently transfected with plasmids encoding firefly and Renilla luciferase for 18 h in transfection medium. Cells were washed and incubated in serum-free medium for 1 h, washed and incubated with the indicated concentration of TNF-α for 4 h and processed to determine LUC activities as described in *Experimental Procedures*. Results were expressed as the mean ± SE (n=3) ratio of firefly:Renilla LUC activity normalized to the untreated control. All TNF-α treated cells (EV and hHARE) were significantly different than untreated control; ****, $p < 0.0001$.

Figure S3: Sequence alignment of human, mouse and rat 190-HARE proteins. Numbering is based on the full-length Stab2 proteins for human (top line; NP_060034.9), mouse (middle line; NP_619614.1) and rat (bottom line; NP_001233286.1 and ADM89077.2). Important features of the proteins are indicated by different colors: the HA-binding Link domains (purple), membrane domains (blue) and cytoplasmic domains (green). Asterisks indicate positions with identical amino acids. The rat Stab2 gene is not completely annotated and the upstream region may be missing some sequences.

Figure S4. DMSO suppresses TNF-α or HA-induced NF-κB activation. Cells expressing hHARE (black bars) or EV (white bars) were transiently transfected with firefly and Renilla luciferase plasmids, incubated for 18 h, washed,and incubated in serum-free medium for 1 h. The washed cells were incubated with 128 mM DMSO (1 %) for 30 min and then with 0.5 ng/ml TNF-α (A) or 50 nM HA (B) for 4 h. Cells were processed to measure LUC activities as described in *Experimental Procedure*. Values are the mean ± SE (n=9) ratio of firefly:Renilla LUC activity normalized to untreated control: ****, $p < 0.0001$.

Figure S5. HARE binds small HA oligosaccharides. Purified 190-hHARE ecto-domain was subjected to SDS-PAGE and electro-blotted to nitrocellulose as described by Harris and Weigel (*Glycobiol*. 18: 638-648, 2008). Separate nitrocellulose strips were incubated with the indicated size oHA (10-20 sugars long) for 2 h at 4°C. Oligosaccharides were synthesized, end-labeled to the same specific radioactivity (using UDP-[^{3}H]GlcUA and PmHAS), and sizes were confirmed as described by Wei and DeAngelis (*J. Biol. Chem*. 279: 42345-9, 2004). A. The strips were washed with TBST three times for 10 min each, air dried and exposed to Kodak BioMax MS film for 5 days at -80°C. B. The developed film was scanned to digitize band images and their integrated densitometry values were corrected for background and then normalized to the IDV of the 10-mer set as 1.0.

Figure S1

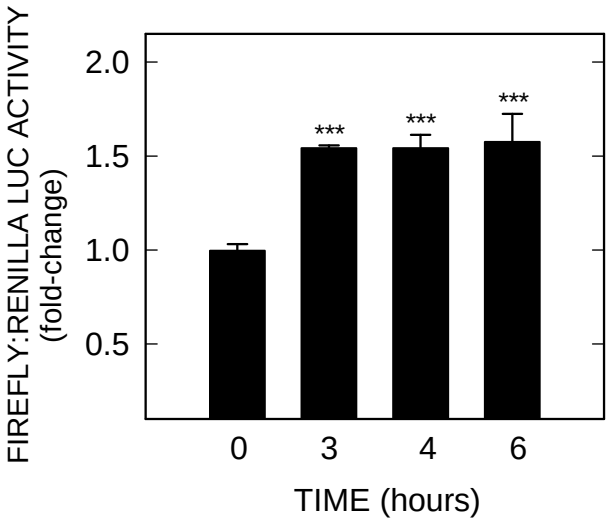
FIREFLY:RENILLA LUC ACTIVITY
(fold-change)
2.0
1.5
1.0
0.5
***
***
***
0
3
4
6
TIME (hours)

Figure S2

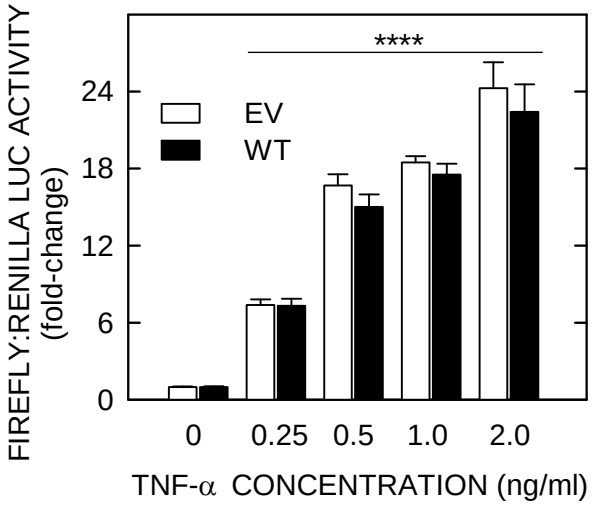
FIREFLY:RENILLA LUC ACTIVITY
(fold-change)
****
EV
WT
24
18
12
6
0
0
0.25
0.5
1.0
2.0
TNF-α CONCENTRATION (ng/ml)

Figure S3. 190-HARE Alignment: human (top), mouse (middle), rat (bottom)

```
SLPNLLMRLEQMPDYSIFRGYIIQYNLANAIEAADAYTVFAPNNNAIENYIREKKVLSLE  1195
SLPSLLTRLEQMPDYSIFRGYIIHYNLASAIEAADAYTVFVPNNEAIESYIREKKATSLK  1203
SLPSLLTRLEQMPDYSIFRGYIIHYNLASAIESADAYTVFVPNNEAIENYIREKKATSLK  1183
*** ** ***************** **** *** ******* *** *** ******  **

EDVLRYHVVLEEKLLKNDLHNGMHRETMLGFSYFLSFFLHNDQLYVNEAPINYTNVATDK  1255
EDILQYHVVLGEKLLRNDLHNGMHRETMLGFSYLLAFFLHNDQLYVNEAPINYTNVATDK  1263
EDILRYHVVLGEKLLKNDLHNGMHRETMLGFSYLLAFFLRNDQLYVNEAPINYTNVATDK  1243
** * ***** **** ***************** * *** ********************

GVIHGLGKVLEIQKNRCDNNDTTIIRGRCRTCSSELTCPFGTKSLGNEKRRCIYTSYFMG  1315
GVIHGLEKVLEIKKNRCDNNDTIIVRGKCGKCSQQTLCPLETKPL-SETRKCIYSVYFMG  1322
GVIHGLEKVLEIQKNRCDNNDTIIVRGECGKCSQQAPCPLETKPL-RETRKCIYSIYFMG  1302
****** ***** ********* * ** *  **    **  ** *  * * ***  ****

RRTLFIGCQPKCVRTVITRECCAGFFGPQCQPCPGNAQNVCFGNGICLDGVNGTGVCECG  1375
KRSIFIGCQLQCVRTIITSACCAGFFGPQCQACPGKGQNVCSGNGFCLDGVNGTGTCECE  1382
KRSVFIGCQPQCVRTIITRACCAGFFGPQCQACPGRGQNVCSGNGFCLDGVNGTGTCQCG  1362
    *****  **** **  *********** ***  **** *** ********* * *

EGFSGTACETCTEGKYGIHCDQACSCVHGRCNQGPLGDGSCDCDVGWRGVHCDNATTEDN  1435
QGFNGTACETCTEGKYGIHCDQACSCVHGRCNQGPSGDGSCDCDVGWRGVKCDSEITTDN  1442
LGFNGTACETCTEGKYGIHCDQACSCVHGRCSQGPLGDGSCDCDVGWRGVKCDMEITTDN  1422
 ** ************************** *** ************** **   * **

CNGTCHTSANCLTNSDGTASCKCAAGFQGNGTICTAINACEISNGGCSAKADCKRTTPGR  1495
CNGTCHTSANCLLDPDGKASCKCAAGFQGNGTVCTAINACEISNGGCSAKADCKRTIPGS  1502
CNGTCHTSANCLLDPDGKASCKCAAGFRGNGTVCTAINACETSNGGCSTKADCKRTTPGN  1482
************   ** ********* **** ******** ************** **

RVCTCKAGYTGDGIVCLEINPCLENHGGCDKNAECTQTGPNQAACNCLPAYTGDGKVCTL  1555
RVCVCKAGYTGDGIVCLEINPCLENHGGCDRHAECTQTGPNQAVCNCLPKYTGDGKVCTL  1562
RVCVCKAGYTGDGIVCLEINPCLENHGGCDRNAECTQTGPNQAVCNCLPKYTGDGKVCSL  1542
*** *************************  *********** ***** ******** *

INVCLTKNGGCSEFAICNHTGQVERTCTCKPNYIGDGFTCRGSIYQELPKNPKTSQYFFQ  1615
INVCLTNNGGCSPFAFCNHTEQDQRTCTCKPDYTGDGIVCRGSIHSELPKNPSTSQYFFQ  1622
INVCLTNNGGCSPFAFCNYTEQDQRICTCKPDYTGDGIVCRGSIYGELPKNPSTSQYFFQ  1602
****** ***** ** ** * *  ******* * ***  *****  ****** *******

LQEHFVKDLVGPGPFTVFAPLSAAFDEEARVKDWDKYGLMPQVLRYHVVACHQLLLENLK  1675
LQEHAVQELAGPGPFTVFVPSSDSFNSESKLKVWDKQGLMSQILRYHVVACQQLLLENLK  1682
LQEHAVRELAGPGPFTVFAPLSSSFNHEPRIKDWDQQGLMSQVLRYHVVGCQQLLLDNLK  1662
**** *  * ******** * *  *  *   * *** *** * ****** * **** ***

LISNATSLQGEPIVISVSQSTVYINNKAKIISSDIISTNGIVHIIDKLLSPKNLLITPKD  1735
VITSATTLQGEPISISVSQDTVLINKKAKVLSSDIISTNGVIHVIDTLLSPQNLLITPKG  1742
VTTSATTLQGEPVSISVSQDTVFINNEAKVLSSDIISTNGVIHVIDKLLSPKNLLITPKD  1722
    ** *****  ***** ** **  **  *********  * ** **** *******

NSGRILQNLTTLATNNGYIKFSNLIQDSGLLSVITDPIHTPVTLFWPTDQALHALPAEQQ  1795
ASGRVLLNLTTVAANHGYTKFSKLIQDSGLLKVITDPMHTPVTLFWPTDKALQALPQEQQ  1802
ALGRVLQNLTTVAANHGYTKFSKLIQDSGLLSVITDSIHTPVTVFWPTDKALEALPPEQQ  1782
  ** * **** * * ** *** ******** ****  ***** ***** ** *** ***

DFLFNQDNKDKLKEYLKFHVIRDAKVLAVDLPTSTAWKTLQGSELSVKCGAGRDIGDLFL  1855
DFLFNEDNKDKLKAYLKFHVIRDTMALASDLPRSASWKTLQGSELSVRCGTGSDVGELFL  1862
DFLFNQDNKDKLKSYLKFHVIRDSKALASDLPRSASWKTLQGSELSVRCGTGSDIGELFL  1842
***** ******* *********   ** *** *  ********** ** * * * ***
```

```
NGQTCRIVQRELLFDLGVAYGIDCLLIDPTLGGRCDTFTTFDASGECGSCVNTPSCPRWS  1915
NGQMCRIIQRRLLFDGGVAYGIDCLLMDPTEGGRCDTFTTFNIPGECGSCFSTPRCPLQS  1922
NEQMCRIIQRGLLFDVGVAYGIDCLLMNPTLGGRCDTFTTFDIPGECGSCIFTPRCPLKS  1902
* * *** ** **** ********** *** **********   ******  ** **  *

KPKGVKQKCLYN-LPFKRNLEGCRERCSLVIQIPRCCKGYFGRDCQACPGGPDAPCNNRG  1974
KPKGVRKKCIYNPLPFRRDVEGCQNLCTLVVHVPRCCSGYFMPDCQACPGGPDTPCNNRG  1982
KPKGVKKKCIYNPLPFRRNVEGCQNLCTLVIQTPRCCHGYFMPDCQACPGGPDTPCNNRG  1962
*****  ** ** *** *  ***   * **   **** ***  ********** ******

VCLDQYSATGECKCNTGFNGTACEMCWPGRFGPDCLPCGCSDHGQCDDGITGSGQCLCET  2034
MCYDQYKPTGQCQCHTGFNGTACELCLPGRFGPDCQPCGCSEHGQCDEGITGSGQCLCEA  2042
MCRDLYTPMGQCLCHTGFNGTACELCWHGRFGPDCQPCSCSEHGQCDEGITGSGECLCET  2082
 * * *   * * * ********* *  ******* ** ** ***** ****** ****

GWTGPSCDTQAVLPAVCTPPCSAHATCKENNTCECNLDYEGDGITCTVVDFCKQDNGGCA  2094
GWTGRFCDAPTVVIPVCIPACSMHATCMENNTCVCNLNYEGDGITCTVVDFCKQNNGGCA  2102
GWTGRFCDTPTAVIPVCTPACSVHATCTENNACVCNLNYEGDGLTCTVVDFCKQNNGGCA  2082
****  **       ** * ** **** *** * *** ***** ********** *****

KVARCSQKGTKVSCSCQKGYKGDGHSCTEIDPCADGLNGGCHEHATCKMTGPGKHKCECK  2154
KVAKCSQKGTQVSCSCQKGYKGDGHSCTEIDPCANGVNGGCHEHATCRMTGPGKQKCECK  2162
KVAKCSQKGTQVSCSCKKGYKGDGYSCIEIDPCADGVNGGCHEHATCRMTGPGKHKCECK  2142
*** ****** ***** ******* ** ****** * ********** ****** *****

SHYVGDGLNCEPEQLPIDRCLQDNGQCHADAKCVDLHFQDTTVGVFHLRSPLGQYKLTFD  2214
SHYVGDGRDCEPEQLPLDRCLQDNGQCHPDANCVDLHFQDTTVGVFHLRSPLGQYKLTFD  2222
SHYVGDGVDCEPEQLPLDRCLQDNGQCHPDASCADLHFQDTTVGVFHLRSPLGQYKLTFD  2202
*******  ******* ********** ** * *************************

KAREACANEAATMATYNQLSYAQKAKYHLCSAGWLETGRVAYPTAFASQNCGSGVVGIVD  2274
KAKEACAKEAASIATYNQLSYAQKAKYHLCSAGWLESGRVAYPTIYASKKCAN-IVGIVD  2281
KAKEACAKEAATIATYNQLSYAQKAKYHLCSAGWLESGRVAYPTTYASQKCGANVVGIVD  2262
** **** ***  ********************** *******  **  *    *****

YGPRPNKSEMWDVFCYRMKDVNCTCKVGYVGDGFSCSGNLLQVLMSFPSLTNFLTEVLAY  2334
YGTRTNKSEMWDVFCYRMKDVNCTCKAGYVGDGFSCNGNLLQVLMSFPSLTNFLTEVLVF  2341
YGSRANKSEMWDVFCYRMKDVNCTCKAGYVGDGFSCSGNLLQVLMSFPSLTNFLTEVLAF  2322
** * ******************** ********* ********************

SNSSARGRAFLEHLTDLSIRGTLFVPQNSGLGENETLSGRDIEHHLA--NVSMFFYNDLV  2392
SRSSAQGRAFLKHLTDLSISGTLFVPQNSGLPKNKSLSGRDIEHHLTNVNVS--FYDDLV  2399
SKSSARGQAFLKHLTDLSIRGTLFVPQNSGLPGNKSLSGRDIEHHLTNVNVS--FYNDLV  2380
* *** * *** ******* ***********  *  **********   ***  ** ***

NGTTLQTRLGSKLLITASQDPLQPTETRFVDGRAILQWDIFASNGIIHVISRPLKAPPAP  2452
NGTVLKTRLGSQLLITSSQDQLH-QEARFVDGRAILQWDIIASNGVLHIISEPLKAPPTA  2458
NGTFLRTMLGSQLLITSSQDQLH-QETRFVDGRSILQWDIIAANGILHIISEPLRAPPTA  2439
*** * * *** **** *** *   * ****** ****** * **  * ** ******

VTLTHTGLGAGIFFAIILVTGAVALAAYSYFRINRRTIGFQHFESEEDINVAALGKQQPE  2512
ATAAHSGLGTGIFCAVVLVTGAIALAAYSYFRLNQRTTGFRRFESEDDIDALAFGKQQPE  2518
ATAAHSGLGTGIFCAVVLVTGAIALAAYSYFRLKQRTTGFQRFESEEDIDVLAFGKQQPK  2499
 *  * *** *** *  ***** *********   ** **  **** **     *****

NISNPLYESTTSAPPEPSYDPFTDSEERQLEGNDPLRTL    2551
SITNPLYETSTPAAPEPSCDPFTDSGERELENSDPLGALRS  2559
NIANPLYETSAPAPPESSCDPFTDPGEQDLEDSDPLGALRS  2540
 * *****    * ** * *****  *  **  ***  *
```

Figure S4

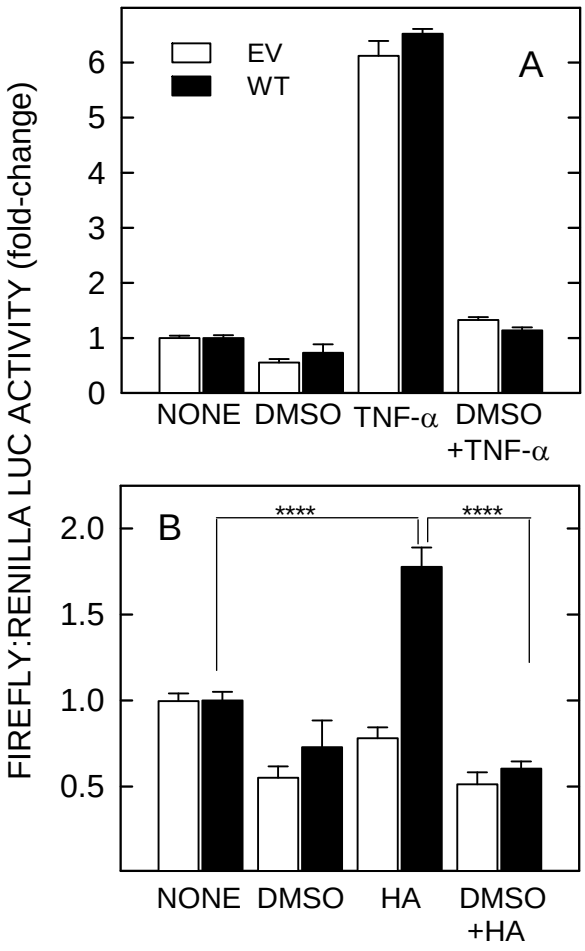
EV
WT
A
FIREFLY:RENILLA LUC ACTIVITY (fold-change)
0
1
2
3
4
5
6
NONE
DMSO
TNF-α
DMSO +TNF-α
B
****
****
0.5
1.0
1.5
2.0
NONE
DMSO
HA
DMSO +HA

Figure S5

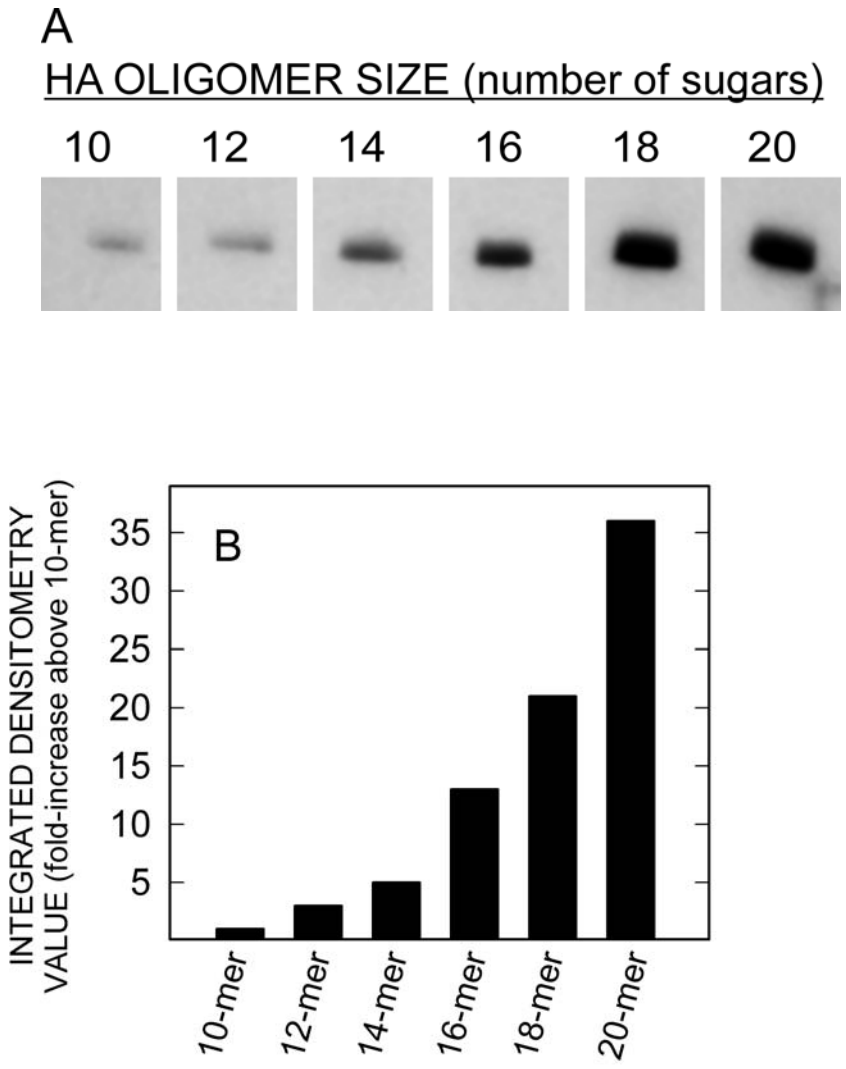
A
HA OLIGOMER SIZE (number of sugars)
10
12
14
16
18
20
B
INTEGRATED DENSITOMETRY VALUE (fold-increase above 10-mer)
35
30
25
20
15
10
5
10-mer
12-mer
14-mer
16-mer
18-mer
20-mer